

Chk2 prevents mitotic exit when the majority of kinetochores are unattached

Eleni Petsalaki and George Zachos

Department of Biology, University of Crete, Heraklion 70013, Greece

The spindle checkpoint delays exit from mitosis in cells with spindle defects. In this paper, we show that Chk2 is required to delay anaphase onset when microtubules are completely depolymerized but not in the presence of relatively few unattached kinetochores. Mitotic exit in Chk2-deficient cells correlates with reduced levels of Mps1 protein and increased Cdk1–tyrosine 15 inhibitory phosphorylation. Chk2 localizes to kinetochores and is also required for Aurora B–serine 331 phosphorylation in nocodazole or unperturbed early prometaphase.

Serine 331 phosphorylation contributed to prometaphase accumulation in nocodazole after partial Mps1 inhibition and was required for spindle checkpoint establishment at the beginning of mitosis. In addition, expression of a phosphomimetic S331E mutant Aurora B rescued chromosome alignment or segregation in Chk2-deficient cells. We propose that Chk2 stabilizes Mps1 and phosphorylates Aurora B–serine 331 to prevent mitotic exit when most kinetochores are unattached. These results highlight mechanisms of an essential function of Chk2 in mitosis.

Introduction

The spindle checkpoint delays exit from mitosis until all sister kinetochores attach to microtubules emanating from opposing spindle poles. The checkpoint signal is generated by kinetochores that lack attachment to spindle microtubules but also by lack of tension across attached sister kinetochores (Nezi and Musacchio, 2009; Foley and Kapoor, 2013). Spindle checkpoint defects are associated with chromosomal instability, aneuploidy, and cancer predisposition (Foley and Kapoor, 2013).

Components of the spindle checkpoint pathway include Mad1, Mad2, BubR1 (Mad3), Bub1, and Bub3 proteins. Recruitment of Mad and Bub proteins to unattached kinetochores is essential to prevent activation of the anaphase-promoting complex/cyclosome (APC/C) and delay exit from mitosis (Nezi and Musacchio, 2009; Foley and Kapoor, 2013). Activated APC/C is an E3 ubiquitin ligase that targets Cyclin B for degradation, leading to inactivation of Cdk1 and initiation of anaphase (Peters, 2002). However, in the presence of an active spindle checkpoint, human cells can “slip” through prolonged mitotic arrest via a slow but continuous degradation of Cyclin B that ultimately drives the cell out of mitosis (Brito and Rieder, 2006). Furthermore, in yeast, Cdk1 can be inactivated by inhibitory phosphorylation of Cdk1 on tyrosine 15 (Y15), rather than by cyclin degradation (Minshull et al., 1996), but whether this

mechanism can operate in mammalian cells in the presence of a fully functional APC/C is still unclear (Brito and Rieder, 2006; Chow et al., 2011).

Mps1 kinase is essential for mitotic arrest and for localization of BubR1 and Mad2 to unattached kinetochores (Abrieu et al., 2001). Mps1 enhances Aurora B kinase activity according to a certain study (Jelluma et al., 2008), and Aurora B activity is required for efficient recruitment of Mps1 to unattached kinetochores (Hewitt et al., 2010; Maciejowski et al., 2010; Santaguida et al., 2010; Saurin et al., 2011). In addition, Mps1 and Aurora B jointly regulate correction of erroneous kinetochore–microtubule attachments (Petsalaki and Zachos, 2013).

Aurora B regulates chromosome alignment and segregation by promoting detachment of misattached microtubules (van der Waal et al., 2012). Aurora B is also involved in the spindle checkpoint; however, its precise role is a matter of active investigation (van der Waal et al., 2012). In higher eukaryotic cells, catalytic activity of Aurora B is required for sustained mitotic arrest in the absence of kinetochore tension (Ditchfield et al., 2003; Lampson and Kapoor, 2005). Furthermore, recent studies have shown that potent inhibition of Aurora B activity weakens the mitotic arrest in the presence of many unattached kinetochores (Santaguida et al., 2011; Saurin et al., 2011; Matson et al., 2012).

Correspondence to George Zachos: gzachos@biology.uoc.gr

Abbreviations used in this paper: APC/C, anaphase-promoting complex/cyclosome; WT, wild type.

© 2014 Petsalaki and Zachos. This article is distributed under the terms of an Attribution-Noncommercial-Share Alike-No Mirror Sites license for the first six months after the publication date (see <http://www.rupress.org/terms>). After six months it is available under a Creative Commons License (Attribution-Noncommercial-Share Alike 3.0 Unported license, as described at <http://creativecommons.org/licenses/by-nc-sa/3.0/>).

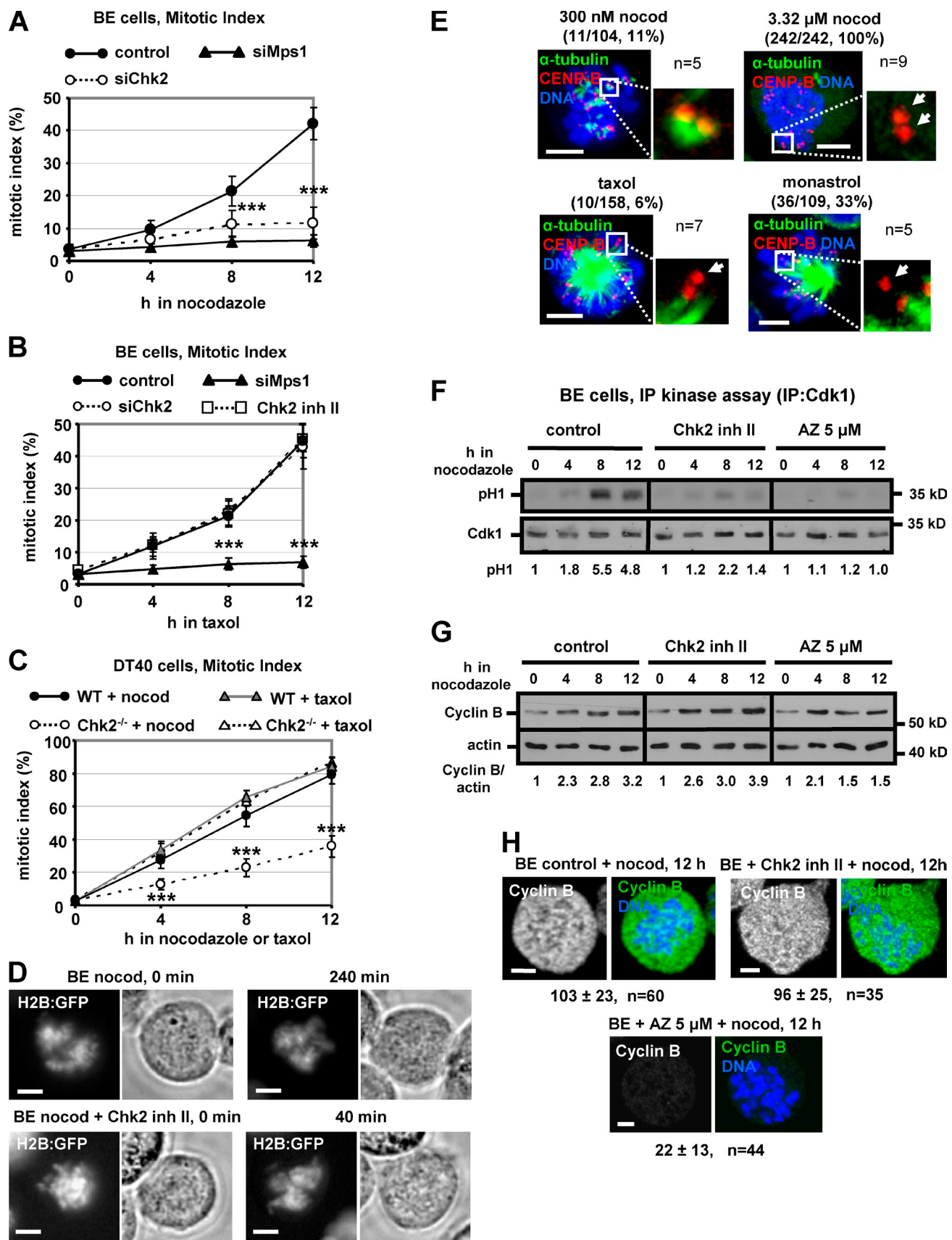


Figure 1. Chk2-deficient cells exit mitosis when the majority of kinetochores are unattached. (A and B) Mitotic index analysis. Cells transfected with negative siRNA (control), Chk2 siRNA (siChk2), Mps1 siRNA (siMps1), or treated with Chk2 inhibitor II were incubated with 3.32 μ M nocodazole (A) or taxol (B). ***, P < 0.001. (C) Wild-type (WT) or Chk2^{-/-} DT40 cells were treated with 3.32 μ M nocodazole (nocod) or taxol. Error bars show the SD from the

Aurora B localizes to centromeres from late prophase until metaphase, and a small population of active Aurora B is also found at kinetochores (Posch et al., 2010; Petsalaki et al., 2011). Chk1 phosphorylates Aurora B–serine 331 (S331) to induce Aurora B kinase activity in “unperturbed” prometaphase (in the absence of spindle poisons) or after treatment of cells with taxol, a drug that dampens microtubule dynamics and primarily interferes with kinetochore tension (Zachos et al., 2007; Petsalaki et al., 2011). However, the kinase that mediates Aurora B–S331 phosphorylation in early mitosis or after microtubule depolymerization by nocodazole has not been previously identified (Petsalaki et al., 2011).

Chk2 is a conserved protein kinase and an effector of the DNA damage response in vertebrate cells (Chen and Poon, 2008). After DNA damage, ATM phosphorylates Chk2 at threonine 68 (T68) within the SQ/TQ cluster domain followed by Chk2 oligomerization, autophosphorylation on threonine 383 (T383) inside the activation loop of the Chk2 catalytic domain, and kinase activation (Lee and Chung, 2001; Ahn et al., 2002; Schwarz et al., 2003). Activated Chk2 phosphorylates cell cycle modulators, including P53 and the Cdk-activating phosphatases Cdc25A and Cdc25C, to induce cell cycle arrest or programmed cell death (Chen and Poon, 2008). Chk2 also phosphorylates Mps1 at threonine 288 (T288) to stabilize Mps1 protein, and Chk2 inhibition diminishes Mps1 levels after DNA damage through a proteasome-independent mechanism (Yeh et al., 2009). In the absence of DNA damage, Chk2 localizes to centrosomes in early mitosis (Tsvetkov et al., 2003) and promotes mitotic spindle assembly, proper chromosome alignment, and segregation through largely undescribed mechanisms (Stolz et al., 2010). However, a role for Chk2 in delaying anaphase onset has not been previously reported. In the present study, we show that Chk2 stabilizes Mps1 protein and phosphorylates Aurora B–S331 to prevent mitotic exit in vertebrate cells when the majority of kinetochores are unattached.

Results

Chk2 delays anaphase onset in response to microtubule depolymerization but not stabilization

To investigate a possible role of Chk2 in the spindle checkpoint, human colon carcinoma BE cells were treated with a relatively high (3.32 μM) concentration of nocodazole to completely depolymerize spindle microtubules (Fig. S1 A) or with 1 μM taxol, which stabilizes microtubules, and the mitotic index was determined. Depletion of Chk2 by siRNA (siChk2) or treatment of cells with the selective Chk2 inhibitor II reduced the mitotic

index after 8–12 h in nocodazole by 48–73% compared with controls (Figs. 1 A and S1 B). In contrast, Chk2-deficient or control cells accumulated in mitosis with similar kinetics in the presence of taxol (Fig. 1 B). Treatment with 2–5 μM of the Mps1 inhibitor AZ3146 completely inhibited human Mps1 kinase activity as judged by phosphorylation of a GST-BLM (9–479) substrate by immunoprecipitated Mps1 in vitro (Leng et al., 2006), whereas lower concentrations of AZ3146 (0.25–1 μM) partially inhibited Mps1 kinase activity (Fig. S1 C). As a positive control, cells depleted of Mps1 by siRNA or treated with 5 μM AZ3146 exhibited reduced mitotic index by 72–86% in the presence of nocodazole or taxol compared with controls (Figs. 1, A and B; and S1 B). Also, Chk2^{-/-} DT40 avian B lymphoma cells in which Chk2 was genetically ablated by gene targeting (Rainey et al., 2008) exhibited decreased prometaphase accumulation in the presence of nocodazole, but not taxol, compared with controls (Fig. 1 C). In addition, treatment of BE cells with high nocodazole did not induce DNA damage as judged by lack of Nbs1 foci on the DNA (Fig. S1 D; Giunta et al., 2010).

Time-lapse analysis of BE cells expressing histone H2B fused to GFP (H2B-GFP) for ≤6 h revealed that a similar percentage (15%) of cells treated with Chk2 inhibitor or controls entered mitosis in the presence of nocodazole as judged by chromosome condensation. Importantly, 12/12 mitotic control cells remained arrested with condensed chromosomes for the duration of the experiment, whereas 12/12 Chk2-deficient cells decondensed their chromosomes after 39 ± 10 min and formed micronuclei (Fig. 1 D and Videos 1 and 2). We conclude that Chk2-deficient cells fail to sustain a delayed anaphase onset in response to high nocodazole.

Chk2 is required for delayed anaphase onset when most kinetochores are unattached

It was recently reported that loss of Chk2 function did not impair mitotic exit in human HCT116 cells treated with 300 nM nocodazole (Stolz et al., 2010), which appears at odds with our observations. Because we use a much higher concentration of nocodazole than the one used by Stolz et al. (2010), we examined the mitotic indices in the same cell type after treatment with relatively high (3.32 μM) or low (300 nM) nocodazole. In the presence of high nocodazole, Chk2 inhibition reduced prometaphase accumulation in HCT116 cells by 53–80% compared with controls (Fig. S1 E). In contrast, Chk2-inhibited or control cells accumulated in prometaphase with similar kinetics after treatment with low nocodazole (Fig. S1 E).

Treatment with low nocodazole was insufficient to completely disrupt microtubule assembly (Fig. S1 A). CHO cells

means from three independent experiments. ***, P < 0.001 compared with WT plus nocodazole. (D) An example of mitotic exit. Cells expressing H2B-GFP were treated with 3.32 μM nocodazole in the absence or presence of Chk2 inhibitor II (inh II) and analyzed by time-lapse microscopy. Phase-contrast (right) and fluorescence images (left) of a cell arrested with condensed chromatin (top row) or a cell that exited mitosis and formed micronuclei (bottom row). Time is from the start of chromatin condensation. See also Video 1 and Video 2. (E) Microtubule–kinetochore attachments in CHO cells. Values in parentheses indicate the frequency of unattached kinetochores from n cells. A 4x magnification of kinetochores is shown. Arrows indicate unattached kinetochores. (F) Cdk1-associated histone H1 kinase activity and Western blot analysis of immunoprecipitated (IP) Cdk1. Cells were treated with 3.32 μM nocodazole in the absence (control) or presence of Chk2 inhibitor II or AZ3146 (AZ). Phosphorylated H1 (pH1) values at 0 h were taken as 1. (G) Western blot analysis of total Cyclin B and actin in cells treated as in F. Values at 0 h were taken as 1. (H) Cyclin B fluorescence in cells treated as in F. Values show mean Cyclin B fluorescence intensity from n cells ± SDs. Bars, 5 μm.

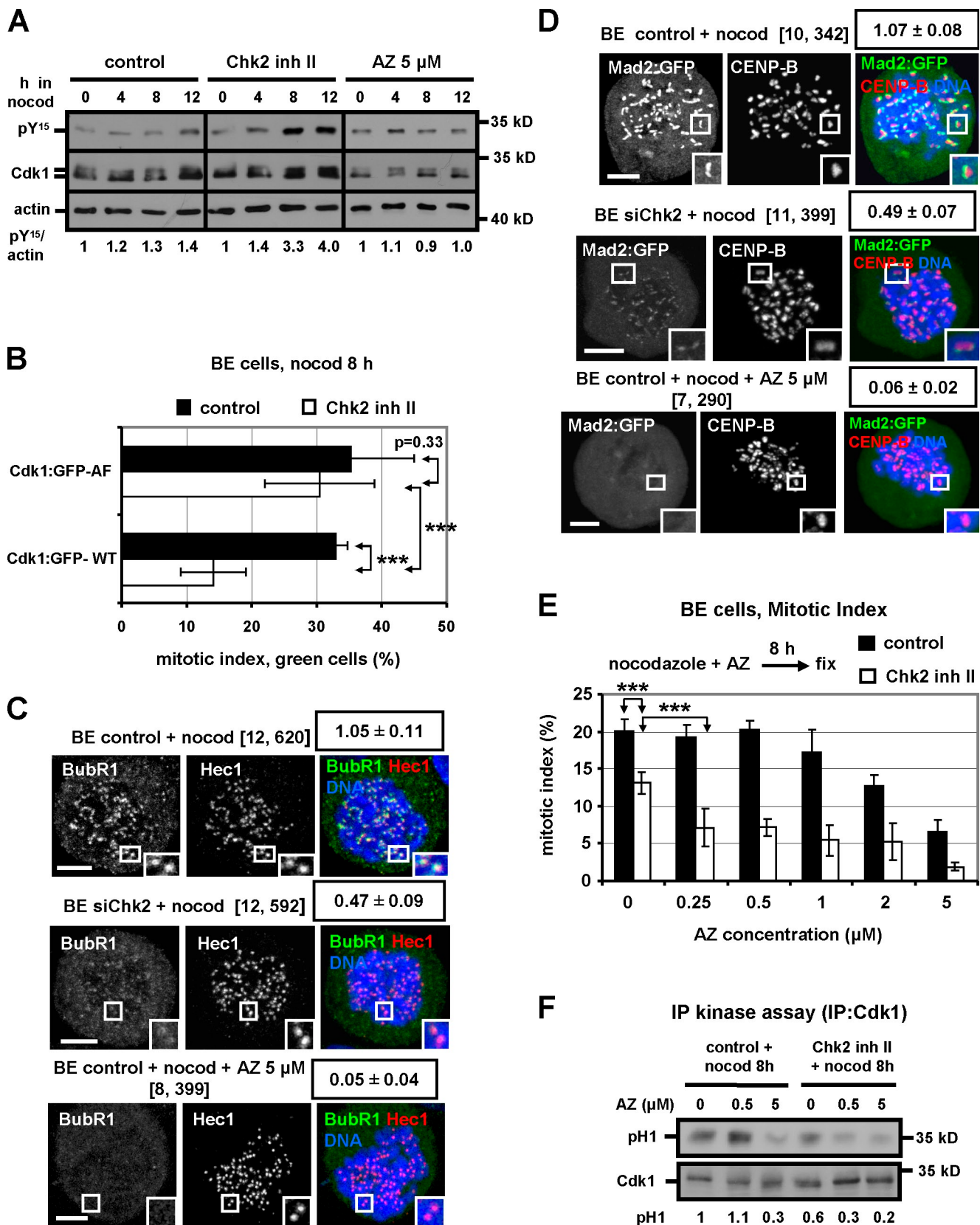


Figure 2. Treatment with AZ3146 exacerbates mitotic exit in Chk2-deficient cells. (A) Western blot analysis of total phosphorylated Y15 (pY¹⁵), Cdk1, and actin. Cells were treated with 3.32 μ M nocodazole (nocod) in the absence (control) or presence of Chk2 inhibitor II (inh II) or AZ3146 (AZ). Values at 0 h were taken as 1. (B) Cells were treated as in A and transfected with AF or WT Cdk1-GFP. Mitotic index shows the percentage of mitotic green cells/total green cells. Error bars show the SD from the means of three independent experiments. ***, P < 0.001. (C) Localization of BubR1. Cells transfected with negative siRNA (control) or Chk2 siRNA (siChk2) were treated with 3.32 μ M nocodazole and MG132 for 4 h in the absence or presence of AZ3146.

treated with low nocodazole exhibited only 11% unattached kinetochores compared with 100% unattached kinetochores in the presence of high nocodazole (Fig. 1 E). As a control, treatment with 1 μ M taxol or 100 μ M monastrol, which inhibits bipolar spindle formation resulted in 6 or 33%, respectively, unattached kinetochores (Fig. 1 E) in agreement with previous findings (Kapoor et al., 2000). Furthermore, Chk2 inhibition diminished prometaphase accumulation by 56% compared with controls after treatment with high nocodazole but not in the presence of low nocodazole, taxol, or monastrol (Fig. S1 F). We propose that Chk2 is required for delayed anaphase onset when the majority of kinetochores are unattached by high nocodazole but not in the presence of relatively few unattached kinetochores after treatment with low nocodazole, taxol, or monastrol. In addition, inhibition of Chk2 after the cells had established a pro-metaphase arrest in high nocodazole did not cause mitotic exit (Fig. S2 A), suggesting that Chk2 is not required for maintaining the arrest.

Chk2-deficient cells exit mitosis through Cdk1-Y15 phosphorylation

Consistent with mitotic exit in the presence of high nocodazole, cells treated with Chk2 inhibitor II or 5 μ M of the Mps1 inhibitor AZ3146 failed to sustain high levels of Cdk1-associated kinase activity after 8–12 h in nocodazole compared with controls (Fig. 1 F). Cells exiting mitosis with an active APC/C are expected to degrade Cyclin B prematurely. Surprisingly, in the presence of nocodazole, Cyclin B accumulated with similar kinetics in Chk2-deficient cells compared with controls (Fig. 1 G). In comparison, Cyclin B levels were diminished after complete Mps1 inhibition by 5 μ M AZ3146 (Fig. 1 G), consistent with improper activation of APC/C. These results were confirmed on a cell by cell basis: In the presence of nocodazole, Chk2-deficient cells in prometaphase exhibited similar levels of Cyclin B-associated fluorescence compared with controls (Fig. 1 H). In comparison, cells treated with 5 μ M AZ3146 exhibited reduced levels of Cyclin B by 79% compared with controls ($P < 0.001$; Fig. 1 H). In addition, time-lapse analysis of cells expressing H2B-GFP and Cyclin B1 fused to mCherry (Cyclin B–mCherry) confirmed that Chk2-deficient cells exit mitosis with high Cyclin B fluorescence in the presence of nocodazole (Fig. S2 B).

Mitotic exit in Chk2-deficient cells treated with high nocodazole was accompanied by increased Cdk1-Y15 phosphorylation (pY15) compared with controls or cells treated with 5 μ M AZ3146 (Figs. 2 A and S2 C). Also, Chk2-inhibited cells treated with nocodazole and enriched in mitosis by shake-off exhibited increased Cdk1-Y15 phosphorylation compared with controls (Fig. S2 D). Furthermore, in the presence of nocodazole, expression of Cdk1-GFP-AF harboring nonphosphorylatable mutations of T14 to alanine and Y15 to phenylalanine, but not wild-type (WT) Cdk1-GFP, rescued prometaphase accumulation in cells

treated with Chk2 inhibitor compared with controls (Fig. 2 B). These results suggest that Chk2-deficient cells exit mitosis through inhibitory phosphorylation of Cdk1-Y15. However, treatment of cells with taxol, monastrol, or low concentration of nocodazole did not induce Cdk1-Y15 phosphorylation compared with controls (Fig. S2 E).

Chk2 is required for optimal localization of BubR1 and Mad2 to kinetochores

Chk2-depleted cells exhibited reduced staining of BubR1 or Mad2-GFP at kinetochores by ~55% after treatment with high nocodazole and proteasome inhibitor MG132, to inhibit mitotic exit, compared with controls ($P < 0.001$; Fig. 2, C and D). In comparison, efficient Mps1 inhibition by 5 μ M AZ3146 diminished BubR1 or Mad2-GFP kinetochore staining by 95% compared with controls ($P < 0.001$; Fig. 2, C and D). BubR1 or Mad2-GFP levels per se were not affected by Chk2 depletion (Fig. S2 F). Also, persistent kinetochore-independent mitotic checkpoint activity by Mad2-GFP overexpression did not rescue prometaphase accumulation in Chk2- or Mps1-deficient cells compared with controls (Fig. S2 G). As a positive control, Mad2-GFP overexpression induced anaphases with lagging chromosomes in the absence of spindle poisons (14/100) compared with cells expressing GFP (4/100; Kabeche and Compton, 2012). These results show that Chk2 is required for optimal localization of BubR1 or Mad2 to kinetochores in response to complete microtubule depolymerization. However, a significant proportion of BubR1 or Mad2 was still detectable at kinetochores in Chk2-deficient cells.

Chk2 and Mps1 cooperate to prevent mitotic exit

To further investigate the role of Chk2 in delayed anaphase onset, we tested the effects from combining Chk2 and Mps1 inhibition in cells treated with high nocodazole. In the absence of Chk2 inhibitor (control), partial Mps1 inhibition by relatively low doses (0.25–1 μ M) of AZ3146 did not significantly reduce the mitotic index compared with 0 μ M AZ3146 (Fig. 2 E). However, in the presence of Chk2 inhibitor, partial Mps1 inhibition further reduced mitotic indices by 43–56% compared with 0 μ M AZ3146 (Fig. 2 E). These results show that partial Mps1 inhibition exacerbates mitotic exit after Chk2 inhibition.

In the presence of nocodazole, incomplete Mps1 inhibition reduced Cdk1 kinase activity and increased Cdk1-Y15 phosphorylation in Chk2-deficient cells compared with controls (Figs. 2 F and 3 A). Also, partial Mps1 inhibition reduced Cyclin B levels in Chk2-deficient prometaphase cells by 50% compared with controls, indicating activation of the APC/C ($P < 0.001$; Fig. 3 B). In addition, low doses of the Mps1 inhibitor diminished BubR1 or Mad2-GFP staining at kinetochores in Chk2-depleted cells by 90–94% compared with controls

(D) Cells expressing Mad2-GFP were treated as in C. (C and D) Boxed values show mean green/red fluorescence intensity \pm SDs. Values in square brackets show kinetochore pairs and number of cells analyzed. Bars, 5 μ m. The insets show 1.7 \times magnification of kinetochores. (E) Mitotic index analysis. Cells treated with 3.32 μ M nocodazole and AZ3146 for 8 h in the absence (control) or presence of Chk2 inhibitor II. Error bars show the SD from the means of three independent experiments. ***, $P < 0.001$. (F) Cdk1-associated histone H1 kinase activity and Western blot analysis of immunoprecipitated (IP) Cdk1 in cells treated as in E. Phosphorylated H1 (pH1) values at first lane were taken as 1.

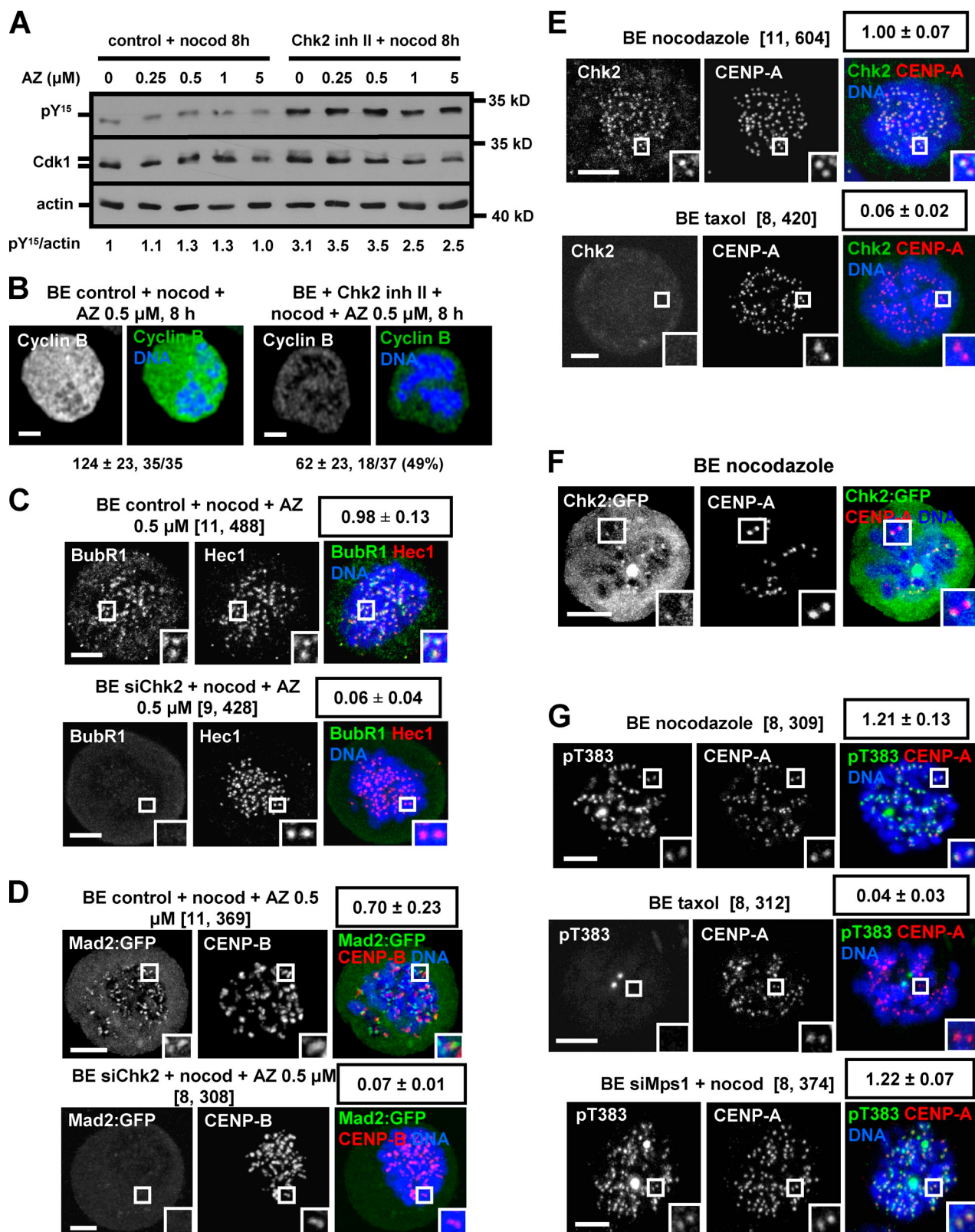


Figure 3. Chk2 is required for BubR1 and Mad2 localization to kinetochores. (A) Western blot analysis of total phosphorylated Y15 (pY¹⁵), Cdk1, and actin. Cells treated with 3.32 μ M nocodazole (nocod) and AZ3146 (AZ) for 8 h in the absence (control) or presence of Chk2 inhibitor II. Values at first lane were taken as 1. (B) Cyclin B fluorescence in cells treated as in A. Values show mean Cyclin B fluorescence intensity \pm SDs. (C) Localization of BubR1. Cells transfected with negative siRNA (control) or Chk2 siRNA (siChk2) were treated with 3.32 μ M nocodazole, MG132, and AZ3146 for 4 h. (D) Cells expressing Mad2:GFP were treated as in C. (E) Localization of Chk2. Cells were treated with 3.32 μ M nocodazole or taxol for 4 h. (F) Cells expressing Chk2-GFP were treated as in E. (G) Localization of phosphorylated Chk2-T383 (pT383). Cells were treated with 3.32 μ M nocodazole or taxol for 4 h or transfected with Mps1 siRNA (siMps1) and treated with 3.32 μ M nocodazole plus MG132 for 4 h. Boxed values show mean green/red fluorescence intensity \pm SDs. Values in square brackets show kinetochore pairs and number of cells analyzed. Bars, 5 μ m. The insets in C–G show 1.7 \times magnification of kinetochores.

($P < 0.001$; Fig. 3, C and D). Collectively, we propose that Chk2 and Mps1 cooperate to promote prometaphase accumulation and spindle checkpoint signaling when most kinetochores are unattached.

Chk2 localizes to kinetochores in high nocodazole or unperturbed early prometaphase

Chk2 localized to kinetochores in cells treated with a high concentration of nocodazole but not taxol (Fig. 3, E and F), and Chk2 was catalytically active as judged by Chk2–phospho-T383 (pT383) staining at kinetochores (Fig. 3 G, pT383). However, Mps1 depletion did not impair Chk2-pT383 kinetochore staining (Fig. 3 G), thus suggesting that Mps1 is not required for localization of active Chk2 to kinetochores.

In the absence of spindle poisons, both total and active Chk2 localized to kinetochores in early prometaphase but not in late prometaphase or metaphase (Fig. 4, A and B). Early prometaphase cells exhibit nuclear envelope breakdown (Fig. S3 A) and condensed chromosomes that do not form a ringlike morphology created in late prometaphase (Magidson et al., 2011). Active Chk2 was also detectable at kinetochores in prophase cells (Fig. S3 A).

Total Chk2 was phosphorylated at T383 after treatment with taxol, nocodazole, or the DNA-damaging agent etoposide (Fig. 4 C). However, exposure to taxol or nocodazole did not result in detectable Chk2-T68 phosphorylation (pT68), although modification of this site was readily observed in cells treated with etoposide (Fig. 4 D). These results indicate that Chk2 is activated through a mechanism that does not involve T68 phosphorylation in cells treated with nocodazole.

Chk2 phosphorylates Aurora B-S331 when microtubules are completely depolymerized by nocodazole

Chk1 phosphorylates Aurora B-S331 in taxol but not in a high concentration of nocodazole (Petsalaki et al., 2011). Because Chk1 and Chk2 can share substrates (Chen and Poon, 2008), we investigated whether Chk2 phosphorylates Aurora B-S331 in nocodazole. Recombinant Chk2 phosphorylated Aurora B in a Chk2 *in vitro* kinase assay, and substrate phosphorylation was markedly reduced after mutation of S331 to alanine (S331A) or Chk2 inhibition compared with WT Aurora B (Fig. 4 E). In high nocodazole, Chk2-depleted cells exhibited diminished Aurora B–phospho-S331 (pS331) staining at kinetochores by 91% compared with controls ($P < 0.001$; Fig. 5 A). However, total Aurora B localized to centromeres in all control and Chk2-depleted cells in prometaphase examined (Fig. 5 B). Also, efficient Mps1 inhibition by treatment with 5 μ M AZ3146 did not impair Aurora B–pS331 staining at kinetochores, showing that S331 phosphorylation is independent of Mps1 kinase activity (Fig. 5 A). Chk2-depleted or control cells exhibited similar levels of phosphorylated Aurora B-S331 at kinetochores in the presence of taxol or low nocodazole (Fig. S3, B and C). In comparison, Chk1 inhibition by UCN-01 diminished Aurora B–pS331 kinetochore staining compared with controls in low nocodazole (Fig. S3 C). We propose that Chk2 is required for

Aurora B–S331 phosphorylation when most kinetochores are unattached by treatment with high nocodazole but not in the presence of relatively few unattached kinetochores by taxol or low nocodazole.

Aurora B-S331 phosphorylation is required for prometaphase accumulation after partial Mps1 inhibition

To investigate the significance of Aurora B–S331 phosphorylation, we used CHO cells expressing 6xMyc-tagged WT, S331A, or S331E mutant Aurora B under control of a tetracycline-induced promoter (Fig. S3, D and E). Cells expressing S331A Aurora B exhibited reduced Myc-associated kinase activity compared with those expressing WT or S331E Aurora B as judged by *in vitro* phosphorylation of Ser10 histone H3 (pH3; Fig. S3 F). However, all three cell lines accumulated in mitosis with similar kinetics in the presence of high nocodazole (Fig. 5 C) in agreement with a previous study (Petsalaki et al., 2011). Chk2 inhibition reduced the mitotic index in cells expressing WT, S331A, or S331E Aurora B by 42–53, 52–64, or 41–57%, respectively, and this was accompanied by an ~54% reduction in Mad2-GFP staining at kinetochores compared with controls without Chk2 inhibitor ($P < 0.001$; Fig. 5, C and D).

Relatively low (0.25–0.5 μ M) concentrations of the Mps1 inhibitor AZ3146 partially inhibited CHO Mps1 kinase activity toward GST-BLM (9–479) *in vitro*, whereas higher (1–5 μ M) concentrations of AZ3146 completely inhibited Mps1 activity (Fig. S3 G). Importantly, treatment with nocodazole in combination with partial Mps1 inhibition reduced prometaphase accumulation by 63–80% and diminished Mad2-GFP staining at kinetochores by 91% in cells expressing S331A Aurora B compared with those expressing WT or S331E Aurora B ($P < 0.001$; Fig. 5, E and F). We propose that Aurora B–S331 phosphorylation is required for prometaphase accumulation and spindle checkpoint signaling in the absence of spindle microtubules after partial Mps1 inhibition.

Chk2 participates in the regulation of Mps1 stability in nocodazole

Inhibition of Mps1 significantly increases its own abundance at kinetochores (Hewitt et al., 2010). In the presence of high nocodazole and 2 μ M of the Mps1 inhibitor AZ3146, Chk2-depleted cells exhibited reduced Mps1-GFP staining at kinetochores by 58% compared with controls ($P < 0.001$; Fig. 6 A). This was not caused by impaired Aurora B–S331 phosphorylation because cells expressing S331A Aurora B exhibited similar levels of Mps1-GFP at kinetochores compared with WT or S331E Aurora B (Fig. S4 A). Instead, Chk2-deficient cells exhibited reduced total levels of transfected Mps1-GFP or endogenous Mps1 proteins by 70–80% compared with controls when most kinetochores were unattached by high nocodazole (Figs. 6 B and S2 E) but not in the presence of taxol, monastrol, or low nocodazole, which produce relatively few unattached kinetochores (Fig. S2 E).

Chk2 phosphorylates Mps1-T288 after DNA damage. In high nocodazole, cells expressing WT Mps1-GFP exhibited increased GFP-associated threonine phosphorylation (pThr) and

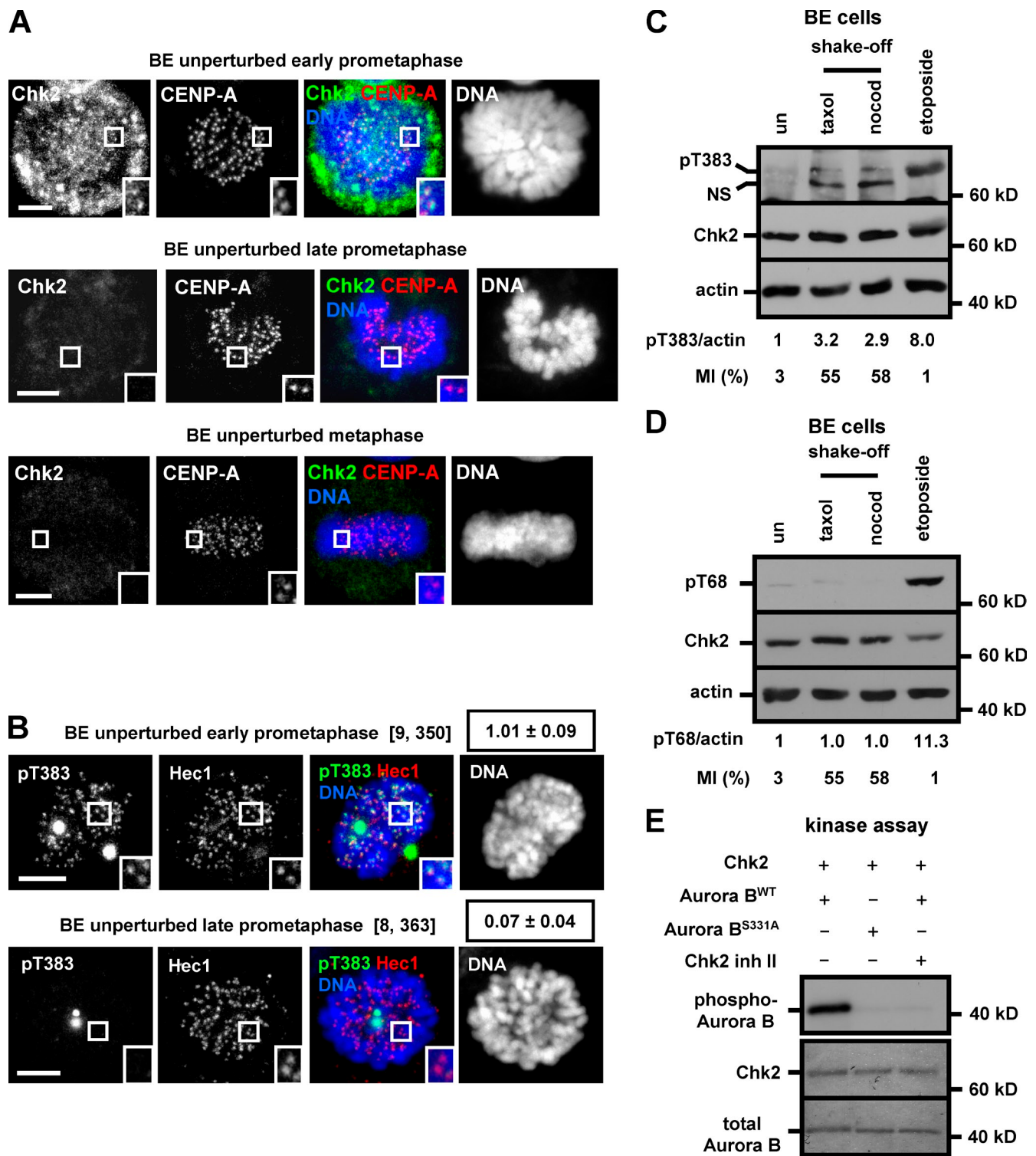


Figure 4. Chk2 localizes to kinetochores in unperturbed early prometaphase. (A) Localization of Chk2. (B) Localization of phosphorylated Chk2-T383 (pT383). Boxed values show mean pT383/Hec1 fluorescence intensity \pm SDs. Values in square brackets show kinetochore pairs and number of cells analyzed. (A and B) Bars, 5 μ m. The insets show 1.7x magnification of kinetochores. (C and D) Western blot analysis of total pT383, Chk2 phospho-T68 (pT68), Chk2, and actin. Cells were untreated (un) or treated with taxol, 3.32 μ M nocodazole (nocod), or etoposide for 8 h followed by shake-off as indicated. Values at untreated were taken as 1. MI, mitotic index; NS, nonspecific. (E) Chk2 in vitro kinase assay. inh II, inhibitor II. (top) Autoradiography analysis of Aurora B substrates. (bottom) Ponceau staining.

total GFP levels compared with those expressing a nonphosphorylatable T288A Mps1-GFP (Fig. 6 C). Furthermore, both T288A and a phosphomimetic T288E Mps1-GFP were resistant to degradation by Chk2 inhibition compared with controls (Fig. 6 D).

We propose that T288 phosphorylation by Chk2 kinase is required for preventing the degradation of Mps1 protein when the checkpoint is activated as a result of a lack of microtubule binding to most kinetochores.

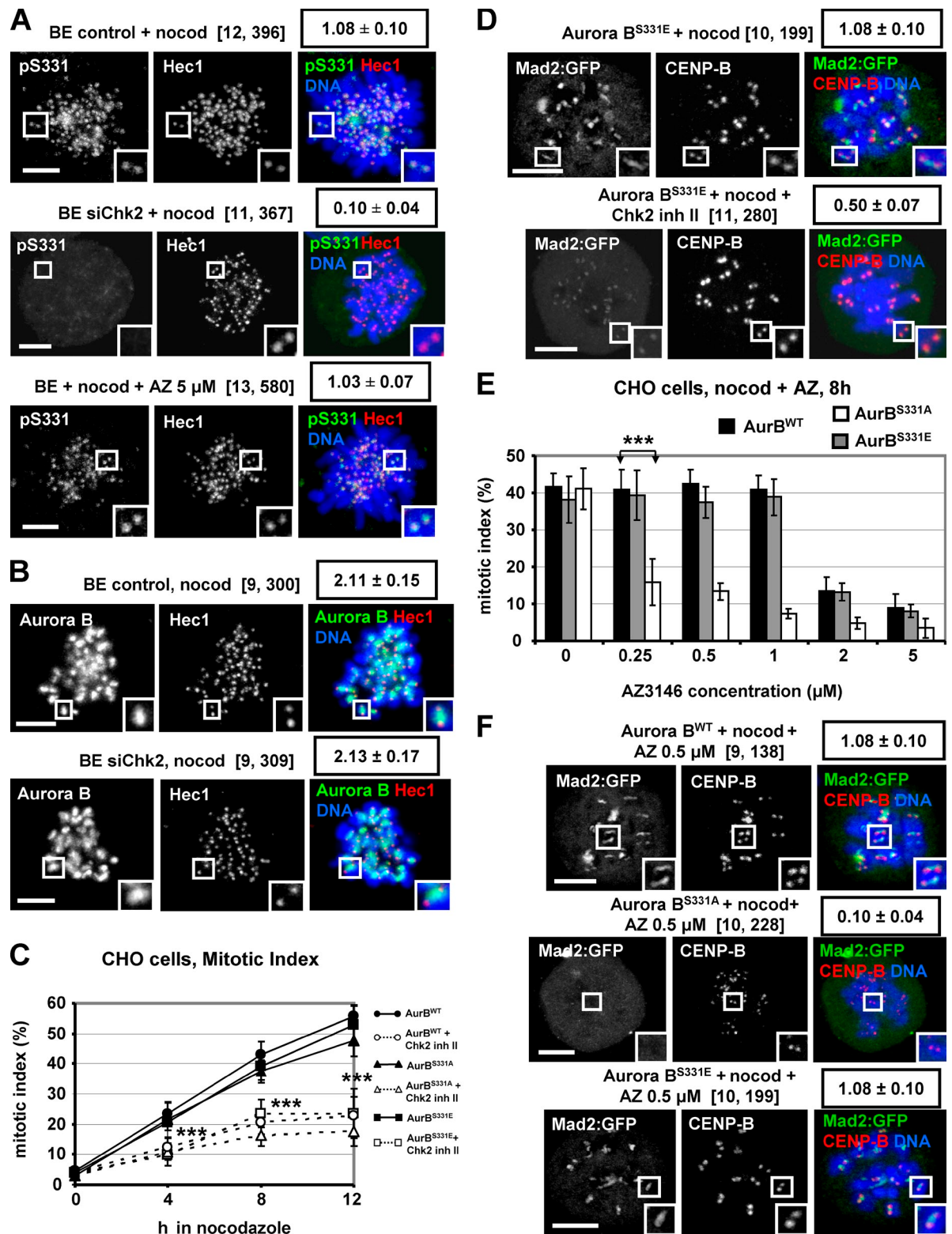


Figure 5. Chk2 is required for Aurora B-S331 phosphorylation in high nocodazole. (A) Aurora B-phospho-S331 (pS331) staining. Cells transfected with negative siRNA (control) or Chk2 siRNA (siChk2) were treated with 3.32 µM nocodazole (nocod) and MG132 for 4 h in the absence or presence of AZ3146 (AZ). (B) Aurora B localization in cells treated as in A. (C) Mitotic index analysis. Tetracycline-induced CHO cells expressing WT, S331A, or S331E Aurora B (AurB) were treated with 3.32 µM nocodazole in the absence or presence of Chk2 inhibitor II (inh II). ***, P < 0.001 compared with cells without Chk2 inhibitor. (D) Tetracycline-induced S331E Aurora B cells expressing Mad2-GFP were treated with 3.32 µM nocodazole and MG132 in the absence or presence of Chk2 inhibitor II for 4 h. (E) Mitotic index analysis. Tetracycline-induced cells expressing WT, S331A, or S331E Aurora B were treated with 3.32 µM nocodazole and AZ3146 for 8 h. Error bars show the SD from the means of three independent experiments. ***, P < 0.001. (F) Tetracycline-induced WT, S331A, or S331E Aurora B cells expressing Mad2-GFP were treated with 3.32 µM nocodazole, AZ3146, and MG132 for 4 h. Boxed values show mean green/red fluorescence intensity ± SDs. Values in square brackets show kinetochore pairs and number of cells analyzed. Bars, 5 µm. The insets in A, B, D, and F show 1.7× magnification of kinetochores.

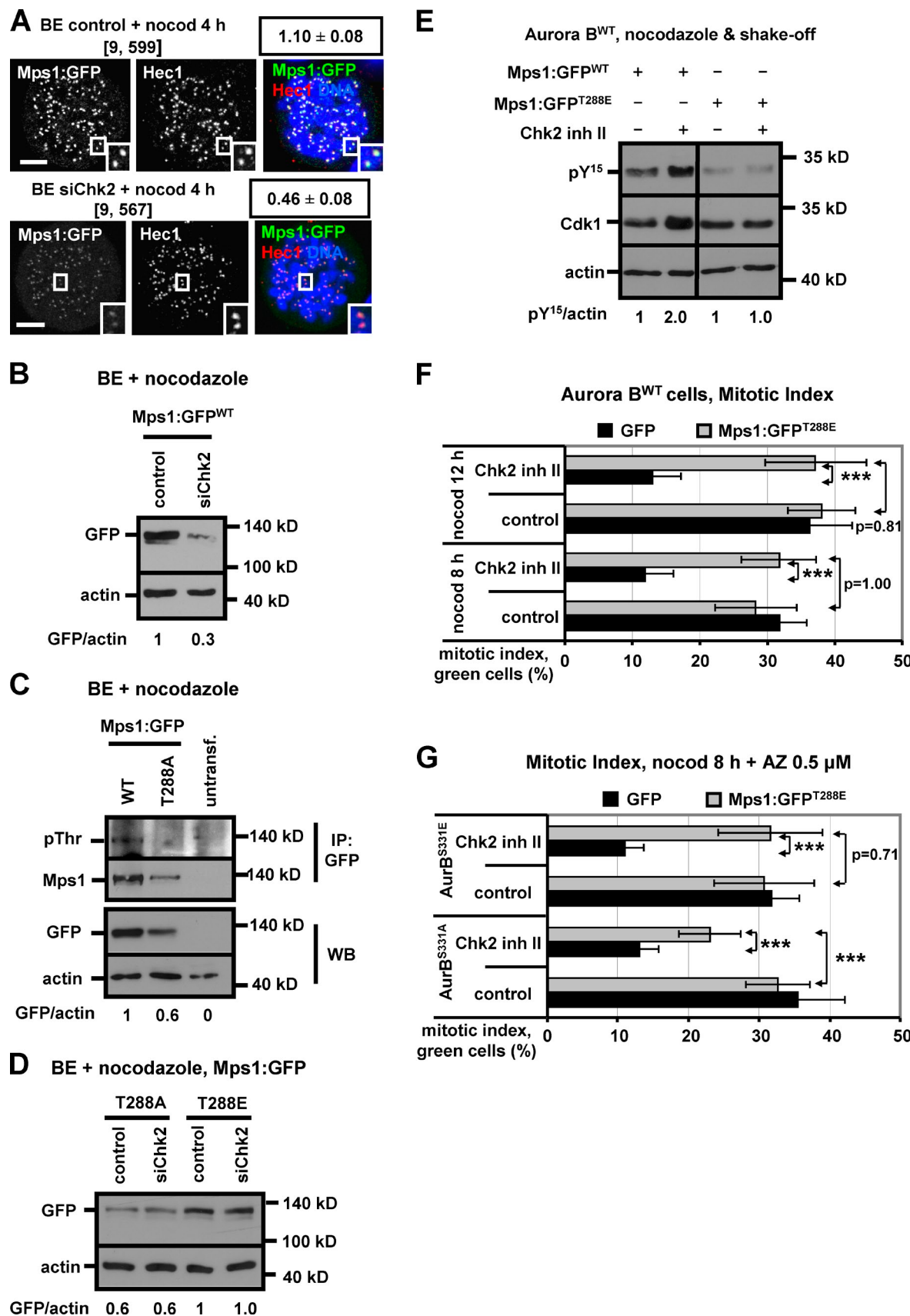


Figure 6. Chk2 is required for Mps1 localization and stability in nocodazole. (A) Cells expressing Mps1-GFP transfected with negative siRNA (control) or Chk2 siRNA (siChk2) were treated with 3.32 μ M nocodazole (nocod) in the presence of AZ3146 (AZ) and MG132 for 4 h. Boxed values show mean Mps1-GFP/Hec1 fluorescence intensity \pm SDs. Values in square brackets show kinetochore pairs and number of cells analyzed. Bars, 5 μ m. Insets

Expression of degradation-resistant Mps1 proteins rescues prometaphase accumulation in Chk2-deficient cells

Cells expressing T288E Mps1-GFP treated with high nocodazole and enriched in mitosis by shake-off exhibited similar levels of Cdk1-Y15 phosphorylation compared with controls (Fig. 6 E). Furthermore, expression of T288E Mps1-GFP, but not WT Mps1-GFP or GFP vector, fully restored prometaphase accumulation in cells treated with Chk2 inhibitor compared with controls (Figs. 6 F and S4 B). Also, cells expressing T288A Mps1-GFP accumulated in prometaphase and exhibited increased levels of Mps1-GFP compared with WT Mps1-GFP cells treated with the Chk2 inhibitor (Fig. S4 C). These results indicate that a critical Mps1 threshold is required for preventing mitotic exit when most kinetochores are unattached.

After treatment with nocodazole in combination with partial Mps1 inhibition by AZ3146, expression of T288E Mps1-GFP partially rescued prometaphase accumulation in cells expressing S331A Aurora B treated with Chk2 inhibitor and completely rescued prometaphase accumulation in cells expressing S331E Aurora B plus Chk2 inhibitor compared with controls or cells expressing GFP (Fig. 6 G). We propose that Chk2 prevents mitotic exit through both Mps1 stabilization and Aurora B-S331 phosphorylation, after partial Mps1 inhibition. In addition, after transfection with WT Mps1-GFP, GFP-associated pThr in cells expressing S331A Aurora B was similar to S331E Aurora B, suggesting that Mps1-T288 phosphorylation is independent of Aurora B-S331 phosphorylation (Fig. S4 D).

Chk2 is required for checkpoint establishment in early mitosis

We also investigated a role of Chk2 in unperturbed mitosis. Chk2-depleted cells exhibited reduced Aurora B-S331 phosphorylation at kinetochores by 87% compared with controls in early prometaphase ($P < 0.001$; Fig. 7 A). In contrast, Chk2-depleted or control cells exhibited similar levels of phosphorylated Aurora B-S331 in late prometaphase (Fig. S4 E).

Furthermore, Chk2-deficient cells in early prometaphase exhibited reduced Cyclin B fluorescence by ~85% compared with controls, indicating untimely activation of the APC/C (Fig. 7 B and not depicted). However, Cyclin B fluorescence was restored to approximately control levels in late prometaphase or metaphase (Fig. 7 B and not depicted). Consistently, Chk2-depleted cells exhibited diminished localization of Mad2-GFP to kinetochores by 93% compared with controls in early, but not in late, prometaphase ($P < 0.001$; Figs. 7 C and S5 A). In anaphase, Cyclin B fluorescence was reduced to background

levels in both Chk2-depleted and control cells (Fig. 7 B), indicating activation of the APC/C upon mitotic exit. These results show that Chk2 is required for Aurora B-S331 phosphorylation and spindle checkpoint establishment in unperturbed early prometaphase. In addition, total levels of Cyclin B or Cdk1 phospho-Y15 in Chk2-deficient cells enriched in mitosis by shake-off were similar to controls (Fig. S5 B).

Aurora B-S331 phosphorylation is required for Mps1 and Mad2 localization to kinetochores in early prometaphase

In the absence of spindle poisons, Chk2-deficient cells exhibited reduced localization of Mps1-GFP to kinetochores by 56% in early prometaphase ($P < 0.001$; Fig. 7 D) and 34% in late prometaphase compared with controls ($P = 0.01$; Fig. S5 C). Also, cells expressing S331A Aurora B exhibited reduced localization of Mps1-GFP or Mad2-GFP to kinetochores by 64 or 91%, respectively, compared with WT or S331E Aurora B in early prometaphase ($P < 0.001$; Fig. 7, E and F). However, total levels of Mps1-GFP were similar in cells expressing WT or S331A Aurora B (Fig. S5 D). We conclude that Chk2 kinase phosphorylation of Aurora B-S331 is required for localization of Mps1 and Mad2 to kinetochores in unperturbed early prometaphase.

Chk2 is required for Mps1 stability in unperturbed mitosis

Chk2-depleted cells enriched in mitosis after release from a thymidine block and shake-off exhibited reduced total levels of Mps1 protein compared with controls (Fig. 8 A). This was not caused by impaired Aurora B-S331 phosphorylation because cells expressing S331E Aurora B exhibited reduced localization of Mps1-GFP to kinetochores after Chk2 inhibition by 62% compared with controls in unperturbed early prometaphase ($P < 0.001$; Fig. 8 B). We propose that Chk2 is required for Mps1 protein stability in unperturbed mitosis.

Expression of S331E Aurora B rescues chromosome alignment and segregation in Chk2-deficient cells

Chk2-depleted BE cells exhibited increased frequency of anaphases with lagging chromosomes (36/100) compared with controls (6/100). Also, in CHO cells, Chk2 inhibition associated with increased chromosome missegregation compared with controls (Fig. S5 E). Also, in the presence of MG132 to block progression of mitosis beyond metaphase, Chk2-deficient cells exhibited increased metaphase chromosome misalignment compared with controls (Fig. S5 F). However, in the presence of

show 1.7 \times magnification of kinetochores. (B) Western blot analysis of total GFP and actin in cells expressing WT Mps1-GFP and treated with 3.32 μ M nocodazole for 8 h. Values at control were taken as 1. (C) Cells expressing WT, T288A Mps1-GFP, or untransfected were treated as in B. (top) Western blot analysis of GFP-associated phosphothreonine (pThr) and Mps1 after GFP immunoprecipitation (IP). (bottom) Western blot (WB) analysis of total GFP and actin. Values at WT were taken as 1. (D) Western blot analysis of total GFP and actin in cells expressing T288A or T288E Mps1-GFP and treated as in B. Values at control T288E were taken as 1. (E) Western blot analysis of total phosphorylated Y15 (pY¹⁵), Cdk1, and actin. Tetracycline-induced CHO WT Aurora B cells expressing WT or T288E Mps1-GFP were treated with 3.32 μ M nocodazole in the absence or presence of Chk2 inhibitor II for 8 h followed by shake-off. Values at samples without Chk2 inhibitor were taken as 1. (F and G) Mitotic index analysis. Tetracycline-induced WT, S331A, or S331E Aurora B cells expressing GFP or T288E Mps1-GFP were treated with 3.32 μ M nocodazole (and AZ3146; G) in the absence (control) or presence of Chk2 inhibitor II (inh II). Mitotic index shows the percentage of mitotic green cells/total green cells. Error bars show the SD from the means of three independent experiments. ***, $P < 0.001$.

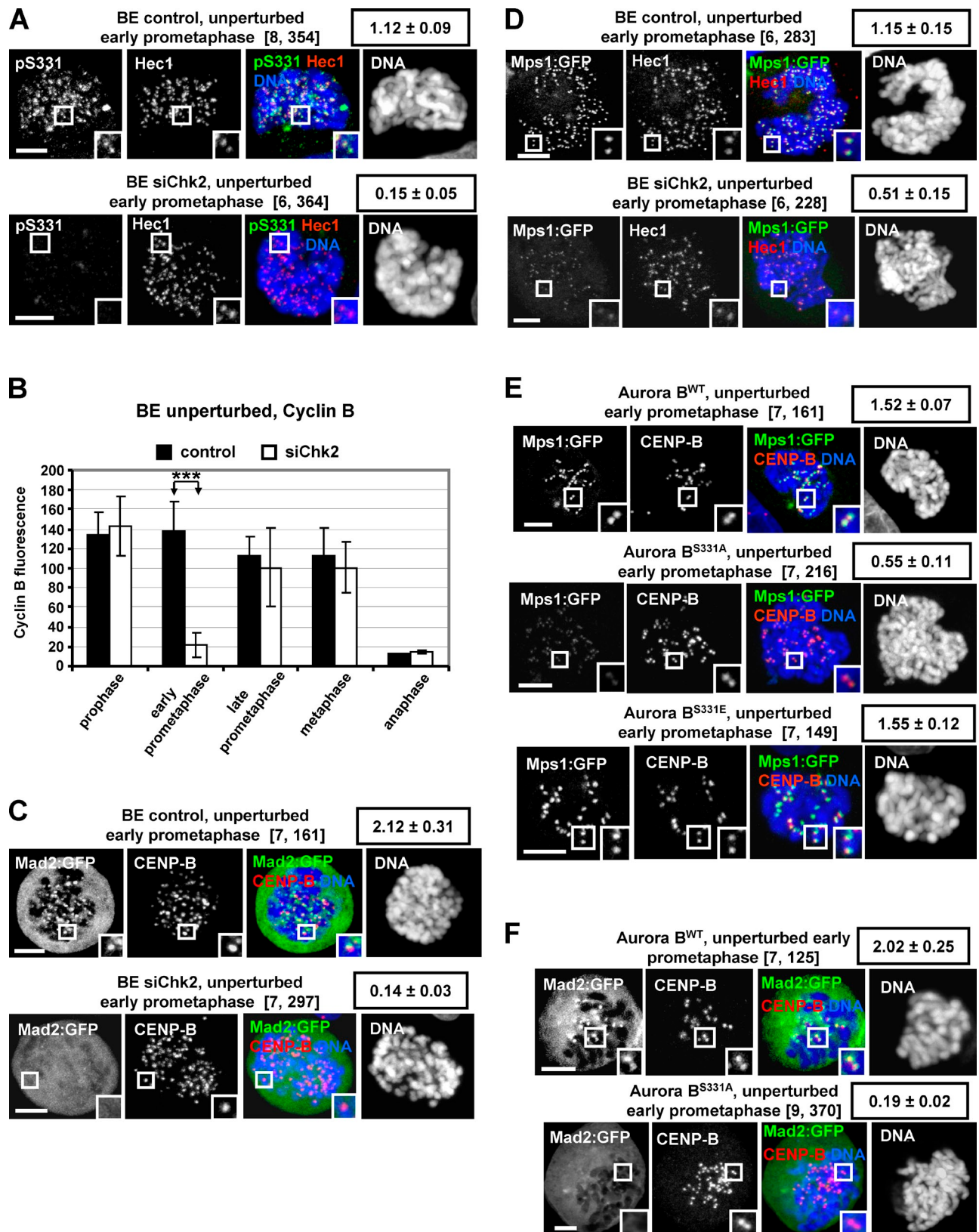


Figure 7. Chk2 is required for spindle checkpoint signaling in unperturbed early prometaphase. (A) Phosphorylated Aurora B-S331 (pS331). Cells were transfected with negative siRNA (control) or Chk2 siRNA (siChk2). (B) Cyclin B fluorescence in cells transfected as in A. ***, P < 0.001. A minimum of 20 cells per treatment was analyzed. Error bars show SDs. (C) Cells expressing Mad2-GFP were treated as in A. (D) Cells expressing Mps1-GFP were transfected as in A and treated with 2 μ M AZ3146 for 1 h. (E) Tetracycline-induced CHO WT, S331A, or S331E Aurora B cells expressing Mps1-GFP were treated with 2 μ M AZ3146 for 1 h. (F) WT or S331A Aurora B cells expressing Mad2-GFP were induced with tetracycline. Boxed values show mean green/red fluorescence intensity \pm SDs. Values in square brackets show kinetochore pairs and number of cells analyzed. Bars, 5 μ m. The insets in A, C, and D-F show 1.7x magnification of kinetochores.

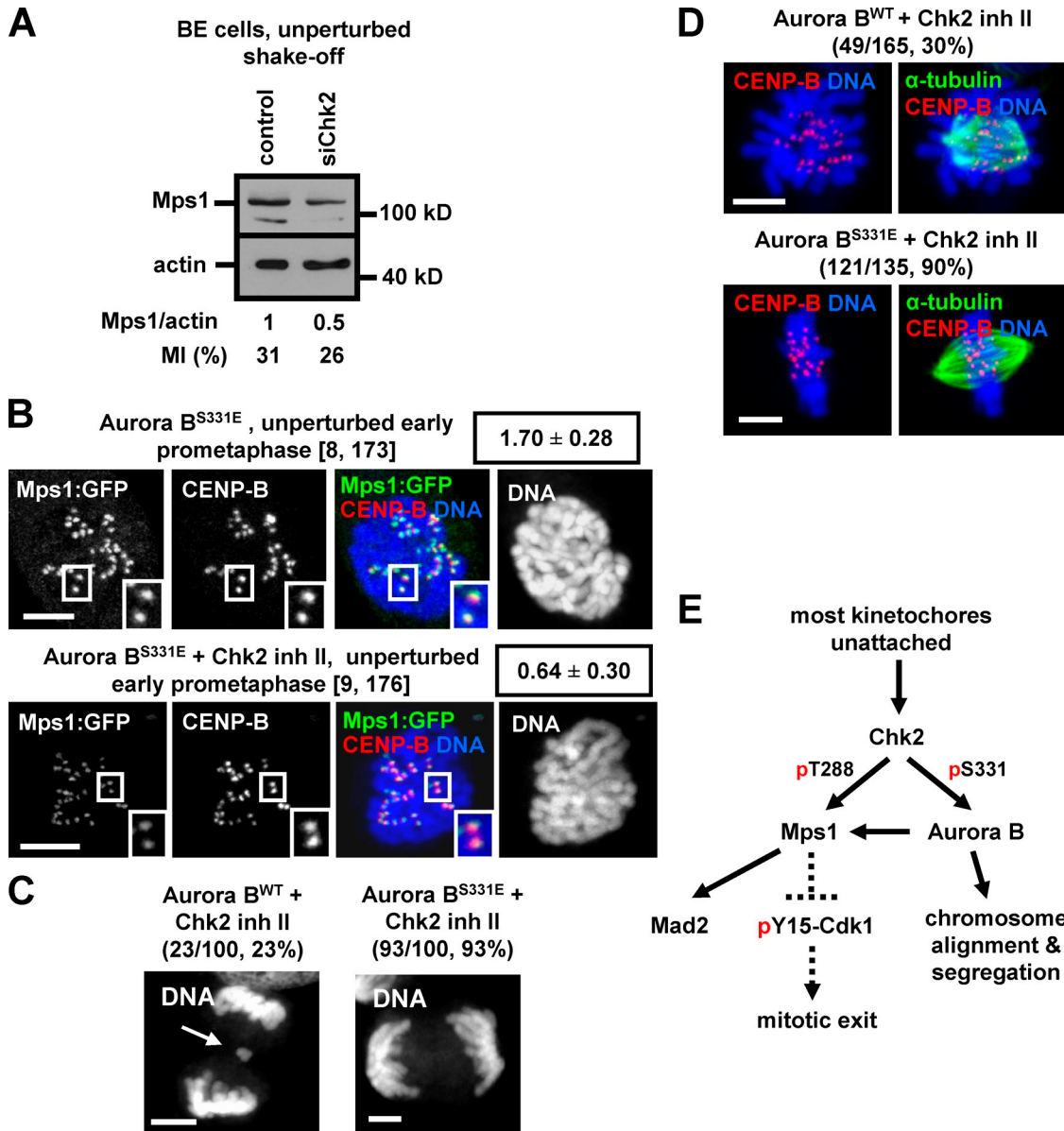


Figure 8. Expression of S331E Aurora B rescues chromosome alignment or segregation after Chk2 inhibition. (A) Western blot analysis of total Mps1 and actin in cells transfected with negative siRNA (control) or Chk2 siRNA (siChk2) followed by shake-off. Values at control were taken as 1. MI, mitotic index. (B) Tetracycline-induced CHO S331E Aurora B cells expressing Mps1-GFP were untreated or treated with Chk2 inhibitor II (inh II) in the presence of 2 μ M AZ3146 for 3 h. Boxed values show mean Mps1-GFP/CENP-B fluorescence intensity \pm SDs. Values in square brackets show kinetochore pairs and number of cells analyzed. Insets show 1.7 \times magnification of kinetochores. (C and D) Tetracycline-induced WT or S331E Aurora B cells were treated with Chk2 inhibitor II for 2 h (C) or with Chk2 inhibitor and MG132 for 1 h (D). (C, left) Anaphase with lagging chromatins (indicated by an arrow). (C, right) Normal anaphase. (D, top) Metaphase with misaligned chromosomes. (D, bottom) Normal metaphase. The frequency of cells exhibiting the respective phenotype is shown in parentheses. (E) Model for the role of Chk2 in mitosis. p indicates phosphorylation. Dotted lines indicate prolonged checkpoint activation. Bars, 5 μ m.

Chk2 inhibitor, expression of S331E Aurora B reduced lagging or misaligned chromosomes by 70 or 67%, respectively, compared with WT Aurora B (Figs. 8, C and D; and S5, E and F). We propose that proper chromosome alignment and segregation require Chk2-mediated Aurora B-S331 phosphorylation.

Discussion

Chk2 is an effector of the DNA damage response in vertebrates; however, a role for Chk2 in delayed anaphase onset has not been previously reported. Here, we show that Chk2-deficient

cells fail to prevent mitotic exit when microtubules are completely depolymerized by a high concentration of nocodazole. In contrast, Chk2 is not required for delayed anaphase onset when cells are treated with taxol, monastrol, or low concentration of nocodazole, which generate relatively few unattached kinetochores. Mitotic exit in Chk2-deficient cells associated with increased Cdk1-Y15 phosphorylation and reduced localization of BubR1 or Mad2 to kinetochores compared with controls but not with Cyclin B degradation. Because \sim 50% of BubR1/Mad2 is still detectable at kinetochores in Chk2-deficient cells compared with controls, this level of BubR1/Mad2 may be

sufficient to inhibit the APC/C and prevent Cyclin B degradation (Ditchfield et al., 2003). These results were unexpected because, in the presence of an active spindle checkpoint, mammalian cells have been shown to slip out of mitosis through gradual Cyclin B degradation (Brito and Rieder, 2006). Instead, our data show that Chk2-deficient cells exit mitosis by Cdk1-Y15 phosphorylation, a mechanism previously shown in yeast or human cells that lack a fully functional APC/C (Minshull et al., 1996; Chow et al., 2011). We also show that Chk2-deficient cells treated with nocodazole exhibit reduced Mps1 protein levels compared with controls. Using T288E Mps1 resistant to degradation after Chk2 depletion, we propose that Chk2 prevents Cdk1-Y15 phosphorylation and mitotic exit by stabilizing Mps1.

Catalytically active Chk2 localizes to kinetochores and is required for Aurora B-S331 phosphorylation in high nocodazole or unperturbed early prometaphase. Using CHO cells expressing WT, S331A, or S331E Aurora B, we propose that S331 phosphorylation is required for prometaphase accumulation in the absence of microtubules and with reduced Mps1 activity. This is consistent with recent studies suggesting that Aurora B is implicated in spindle checkpoint signaling in nocodazole when partial inhibition of checkpoint components presumably causes a weakened signal (Santaguida et al., 2011; Matson et al., 2012). We also show that, in the absence of spindle drugs, Aurora B-S331 phosphorylation is required for optimal localization of Mps1 to kinetochores and spindle checkpoint establishment in early prometaphase, consistent with Mps1 activation by Aurora B at the onset of mitosis (Saurin et al., 2011). However, in late prometaphase, Chk2-deficient cells exhibit a functional spindle checkpoint and restored Cyclin B levels compared with controls. Although the mechanism of this is unknown, Cyclin B can be rapidly synthesized in mitosis through cytoplasmic polyadenylation element-binding protein-dependent translation (Malureanu et al., 2010). Chk2 depletion also reduced Mps1 protein levels but did not detectably increase Cdk1-Y15 phosphorylation compared with controls in unperturbed mitosis. It is possible that Mps1 is required to prevent Cdk1-Y15 phosphorylation after prolonged checkpoint activation. In addition, expression of S331E Aurora B rescues chromosome alignment and segregation in Chk2-deficient cells.

On the basis of those findings, we propose the following model for the role of Chk2 in mitosis (Fig. 8 E): In unperturbed early prometaphase or after treatment of cells with a high concentration of nocodazole, the majority of kinetochores are unattached, and Chk2 associates with kinetochores. Activated Chk2 stabilizes Mps1 protein levels, possibly through phosphorylating Mps1-T288 and inhibits Cdk1-Y15 phosphorylation through an Mps1-dependent mechanism to prevent mitotic exit after prolonged checkpoint activation. Furthermore, Chk2 phosphorylates Aurora B-S331 to induce Aurora B kinase activity, and this phosphorylation is required for optimal localization of Mps1 and Mad2 to kinetochores and inactivation of the APC/C at the beginning of mitosis. In addition, Chk2 promotes proper chromosome alignment through Aurora B-S331 phosphorylation. Later in prometaphase, cells progressively form kinetochore-microtubule attachments, and Chk2 dissociates from kinetochores and is dispensable for Aurora B-S331 phosphorylation

and spindle checkpoint establishment. As a result, Chk2-deficient cells exit mitosis upon activation of the APC/C but exhibit increased frequency of chromosome missegregation. Our model raises several important questions regarding the molecular mechanism of Cdk1-Y15 phosphorylation, the mechanism of Chk2 activation in mitosis, and the significance of Chk2 signaling for error correction.

In interphase cells, Cdk1-Y15 phosphorylation is imposed by the Wee1 and Myt1 kinases and requires Cdk1 in complex with Cyclin B (McGowan and Russell, 1993; Mueller et al., 1995b). Potent inhibition of Mps1 inactivates the spindle checkpoint, forcing cells to exit mitosis through Cyclin B degradation (Abrieu et al., 2001; Maciejowski et al., 2010). However, the fact that a Cyclin B-Cdk1 complex is present in Chk2-deficient cells could provide substrates for Wee1 and Myt1 kinases to impose the Cdk1-Y15 phosphorylation (McGowan and Russell, 1993; Mueller et al., 1995b). Because activation of Wee1/Myt1 requires removal of their inhibitory phosphorylation (Tang et al., 1993; Mueller et al., 1995a), one possibility is that reduced BubR1/Mad2 binding to kinetochores in Chk2-deficient cells can lead to a slight reduction of Cdk1 activity perhaps by a small fraction of active APC/C, which in turn is sufficient to turn on some Wee1/Myt1 and start the Cdk1-Wee1/Myt1 feedback loop. Alternatively, a Wee1/Myt1 stimulatory phosphatase that removes the inhibitory phosphorylation of Wee1/Myt1 may become activated in Chk2-deficient cells (Tang et al., 1993).

Chk2-T68 phosphorylation promotes Chk2 kinase activation after DNA damage (Lee and Chung, 2001; Ahn et al., 2002). However, we show that Chk2 is activated in the absence of T68 phosphorylation in mitotic cells, in agreement with a previous study (van Vugt et al., 2010). Because Chk2 overexpression can promote oligomerization and cis- and trans-phosphorylation of regulatory residues (Ahn and Prives, 2002; Schwarz et al., 2003), one possibility is that local enrichment of Chk2 at kinetochores facilitates Chk2 oligomerization and activation without T68 phosphorylation. This mechanism may contribute to spatial regulation of Chk2-dependent processes in mitosis.

Chk2 is required for Aurora B-S331 phosphorylation at the beginning of mitosis, whereas Chk1 is required later in mitosis (Zachos et al., 2007). Although the biological rationale of this scenario is currently unknown, it may reflect different phases of mitosis in which Chk1 and Chk2 are activated. A similar division of labor occurs in the G2 DNA damage checkpoint: Chk1 prevents G2 cells with damaged DNA from entering mitosis, whereas Chk2 is solely responsible for mitotic delay in late G2 cells, which are imminently about to enter mitosis (Rainey et al., 2008).

Diminished Aurora B-S331 phosphorylation in Chk2-deficient cells can induce erroneous kinetochore-microtubule attachments in early mitosis (Petsalaki and Zachos, 2013). Because Chk2-deficient cells exhibit a functional spindle checkpoint in late prometaphase, they can delay anaphase to correct many kinetochore misattachments. This may explain how Chk2-deficient cells apparently segregate the majority of their chromosomes correctly and is consistent with increased duration of unperturbed prometaphase and metaphase in those cells (Stolz et al., 2010). However, because some erroneous (merotelic)

attachments can evade detection from the spindle checkpoint (Cimini, 2008), Chk2-deficient cells can enter anaphase with higher frequency of lagging chromosomes compared with controls. Further experiments are under way to understand the role of Chk2 in error correction.

Materials and methods

Antibodies and plasmids

Mouse monoclonal antibodies against Cdk1 (Cdc2 p34; 17) and Myc (9E10) and rabbit polyclonal antibodies against CENP-B, GFP (FL), Mps1 (tyrosine threonine kinase; C-19; used in Western blotting), Chk2 (H-300; used in immunofluorescence), Cyclin B1 (H-433), phospho-Tyr15 (pCdc2 p34; Tyr15), phospho-histone H3 (Ser10), and Nibrin (Nibrin; H-300) were obtained from Santa Cruz Biotechnology, Inc. Mouse monoclonal anti-BubR1 (8G1; used in Western blotting), mouse monoclonal anti-Mps1 antibody (ab11108; used in immunoprecipitations), rabbit polyclonal anti-Chk2-pT383 (ab59408), rabbit polyclonal anti-pThr (ab9337), and rabbit polyclonal anti-Aurora B (ab2254) antibodies were obtained from Abcam. Mouse monoclonal anti-Chk2 (IC12; used in Western blotting) and rabbit polyclonal antiphospho-Chk2 (Thr68) antibodies were obtained from Cell Signaling Technology. Mouse monoclonal antibodies against α -tubulin (DM1A) and actin (AC-40) were obtained from Sigma-Aldrich, anti-CENP-A (3-19) and anti-Hec1 (9G3.23) were purchased from Genetex, and anti-lamin B2 (E-3) was purchased from Life Technologies. Anti-pS331 antiserum was generated in rabbit by immunization against the phosphorylated peptide pS331 (H2N-CPWVRANS[PO3H2]RRVLPSCONH2) of human Aurora B (Petsalaki et al., 2011). Anti-BubR1 antibody SBR1.1 was generated in sheep by immunization against human GST-BubR1 (2-211) and was a gift from S. Taylor (University of Manchester, Manchester, England, UK; Taylor et al., 2001).

Plasmid pEGFP-N1 coding for GFP under cytomegalovirus promoter was obtained from Takara Bio Inc. and pCyclin B1-mCherry (plasmid 26063) coding for human Cyclin B1 fused to mCherry under cytomegalovirus promoter was from Addgene (Gavet and Pines, 2010). Plasmid Mps1-GFP coding for human Mps1 fused to GFP in pcDNA5/FRT/TO was a gift from S. Taylor (Hewitt et al., 2010), and plasmid Mad2-GFP encoding avian Mad2 fused to GFP in pEGFPN1 vector was from T. Fukagawa (National Institute of Genetics, Shizuoka, Japan; Zachos et al., 2007). pCdc2-GFP-AP coding Cdk1 (Cdc2) in which Thr14 and Tyr15 were mutated to alanine and phenylalanine, respectively, fused to GFP in pLEGFP-N1 vector was from R. Muschel (Oxford Institute for Radiation Oncology, Oxford, England, UK; Fletcher et al., 2002). Plasmid pGEX-4T-1 BLM (1-1,417) coding full-length human BLM fused to GST was a gift from S. Sengupta (National Institute of Immunology, New Delhi, India; Srivastava et al., 2009).

Recombinant and purified proteins

Recombinant histone H1, histone H3, and Chk2 His tag proteins were obtained from EMD Millipore. WT or T1052G (changing S331 to alanine) human Aurora B cDNAs into pET-28a(+) vectors (EMD) were expressed in BL21 (DE3) cells (Agilent Technologies). Proteins were purified using the 6xHis purification kit (B-PER; Thermo Fisher Scientific) and used as substrates in kinase reactions. Human GST-BLM (9-479) protein was expressed in BL21 (DE3) cells and purified using glutathione-agarose beads (Santa Cruz Biotechnology, Inc.).

Mutagenesis, cloning, and generation of cell lines

The Mps1-GFP plasmid (see previous paragraph) was used to generate point mutations A862G, C863A, A864G (numbers refer to human Mps1 cDNA) changing Thr288 to glutamic acid (T288E), or mutation A862G changing Thr288 to alanine (T288A) by site-directed mutagenesis using the mutagenesis kit (QuikChange; Agilent Technologies). To generate plasmid pGEX BLM (9-479) coding GST-BLM (9-479) protein, a BLM fragment containing amino acids 9-479 of human BLM was isolated by PCR using pGEX-4T-1 BLM (1-1,417) as a template, cloned as a BamHI-NotI fragment into the pGEX-4T-1 vector (Addgene), and completely sequenced.

To produce cell lines expressing WT or nonphosphorylatable S331A mutant Aurora B, WT or T1052G (changing S331 to alanine) human Aurora B cDNAs were subcloned as EcoRI-NotI fragments into the 6xMyc-pcDNA3 vector (Invitrogen), excised with BamHI-NotI, and introduced into the pcDNA5/FRT/TO plasmid (Invitrogen) as previously described (Petsalaki et al., 2011). To produce a cell line expressing a phosphomimetic S331 to glutamic acid (S331E) Aurora B, WT 6xMyc-Aurora B

cloned into pcDNA5/FRT/TO vector was used to generate point mutations T991G, C992A, and T993G changing S331 to glutamic acid by site-directed mutagenesis (QuikChange). These vectors were then transfected into CHO cells (T-REx; Invitrogen) stably expressing the tetracycline repressor together with the pTK-Hyg selection vector (Agilent Technologies) conferring resistance to hygromycin (Invitrogen).

To produce human colon carcinoma BE cells stably expressing H2B fused to GFP, the human H2B gene was subcloned as a KpnI-BamHI fragment into the cloning site of pEGFP-N1 (Takara Bio Inc.), and this plasmid was transfected in BE cells together with the pTK-Hyg selection vector. Chk2-deficient avian B lymphoma DT40 cells (Chk2^{-/-}), in which both Chk2 alleles were disrupted by transfection of neomycin or puromycin targeting vectors in pBluescript KS (Agilent Technologies), designed to delete both the Chk2 Forkhead-associated and kinase domains, were a gift from D. Gillespie (Beatson Institute for Cancer Research, Glasgow, Scotland, UK; Rainey et al., 2008).

Cell culture and treatments

BE or HCT116 cells were grown in DMEM (Gibco) containing 10% fetal bovine serum and CHO cells in Ham's F12 (Gibco) supplemented with 10% fetal bovine serum at 37°C in 5% CO₂. DT40 cells were cultured in DMEM containing 10% fetal bovine serum, 1% chicken serum, and 10⁻⁵ M β -mercaptoethanol at 39.5°C in 5% CO₂.

Cells were treated with 3.32 μ M nocodazole (unless otherwise stated), 1 μ M taxol (AppliChem), 10 μ g/ml MG132 (EMD Millipore), 10 μ M Chk2 inhibitor II (EMD Millipore), 10 μ M etoposide (Sigma-Aldrich), 100 μ M monastrol (Sigma-Aldrich), or AZ3146 (Axon Medchem) as appropriate. To induce expression of WT, S331A, or S331E Aurora B transgenes, cells were treated with 17, 30, or 50 ng/ml tetracycline (Sigma-Aldrich), respectively, for 16 h before analysis or further treatment with drugs.

Addition of tetracycline stimulated accumulation of 6xMyc-Aurora B proteins at approximate levels 10-fold higher than the endogenous protein, and this level of expression was shown to disrupt endogenous Aurora B functions while maintaining correct localization of 6xMyc-Aurora B to centromeres (Petsalaki et al., 2011). Negative siRNA or siRNA duplexes designed to repress human tyrosine threonine kinase (Mps1; Thermo Fisher Scientific) or Chk2 (sc29271; Santa Cruz Biotechnology, Inc.) were transfected into BE cells 24 h before analysis using Lipofectamine 2000 (Invitrogen). For expression of GFP proteins, plasmids were transfected into cells in the absence or presence of appropriate siRNA duplexes 24 h before analysis or further treatment with drugs using Lipofectamine 2000.

Cell synchronization and mitotic enrichment

Nocodazole- or taxol-treated cells were enriched in mitosis by shake-off. In the absence of spindle poisons, cells were treated with 2 mM thymidine (Sigma-Aldrich) for 16 h, washed twice with PBS, and released into fresh medium for 10 h before mitotic enrichment by shake-off. Approximately one third of the cells were used to determine mitotic indices by microscopy (see following paragraph), and the remaining were lysed for Western blotting.

Time-lapse imaging

BE cells stably expressing H2B-GFP were seeded onto Petri dishes with a 30-mm glass base (IWAKI; Asahi glass Co., Ltd.). Phase-contrast and fluorescence images were taken every 5–20 min for 6 h using an inverted fluorescence microscope (DMI4000B; Leica) and a 40x Plan Neo 0.6 NA Ph2 objective. Imaging was performed in air, at 37°C in 5% CO₂, using a camera (DFC300FX; Leica) and IM50 acquisition software (Leica). To visualize Cyclin B by time lapse, BE H2B-GFP cells were transfected with plasmid pCyclin B1-mCherry, transferred onto glass base Petri dishes, and analyzed 24 h after transfection.

Indirect immunofluorescence microscopy

To depolymerize the majority of nonkinetochore microtubules and count unattached kinetochores (Fig. 1 E), cells were incubated in ice-cold medium for 15 min at 4°C, prefixed in prewarmed (37°C) 4% paraformaldehyde in Phem buffer (60 mM Pipes, 25 mM Hepes, pH 7.0, 10 mM EGTA, and 4 mM MgSO₄) for 10 s at room temperature, permeabilized in prewarmed (37°C) Phem supplemented with 0.5% Triton X-100 for 5 min at room temperature, fixed in prewarmed (37°C) 4% paraformaldehyde in Phem for 20 min at room temperature, washed twice with PBS, and immunostained (Petsalaki and Zachos, 2013). To measure the percentage of unattached kinetochores, only kinetochores that were clear of the main microtubule mass (in cells treated with taxol or monastrol) were taken into account.

For Aurora B-pS331 or Chk2-pT383 staining, cells were extracted in prewarmed (37°C) Phem buffer supplemented with 0.5% CHAPS and 100 nM microcystin (Sigma-Aldrich) for 5 min at room temperature, fixed with 4% prewarmed (37°C) 4% paraformaldehyde in Phem buffer for 10 min at room temperature, permeabilized in 0.5% Triton X-100 in Phem buffer for 2 min at room temperature, washed twice with PBS, and immunostained as appropriate. For Chk2 staining, cells were fixed in ice-cold methanol for 5 min at -20°C, washed twice with PBS at room temperature, and immunostained.

For all other fluorescence microscopy applications, cells were fixed in 4% paraformaldehyde in cytoskeleton buffer (1.1 M Na₂HPO₄, 0.4 M KH₂PO₄, 137 mM NaCl, 5 mM KCl, 2 mM MgCl₂, 2 mM EGTA, 5 mM Pipes, and 5 mM glucose, pH 6.1) for 5 min at 37°C, permeabilized in 0.5% Triton X-100 in cytoskeleton buffer at room temperature, and immunostained as appropriate (Zachos et al., 2007).

FITC- or rhodamine-TRITC-conjugated secondary antibodies (Jackson ImmunoResearch Laboratories, Inc.) were used as appropriate, DNA was stained with 10 μM TO-PRO-3 iodide (642/661 nm; Invitrogen), and cells were mounted in Vectashield medium (Vector Laboratories). Images were collected using a laser-scanning spectral confocal microscope (TCS SP2; Leica), LCS Lite software (Leica), and a 63x Apochromat 1.40 NA oil objective. The low fluorescence immersion oil (11513859; Leica) was used, and imaging was performed at room temperature. Average projections of image stacks were obtained using the LCS Lite software.

To analyze fluorescence intensities, background readings were subtracted and green/red fluorescence intensities quantified using LCS Lite. The BubR1 and total Aurora B values were normalized against the Hec1 signal, the GFP was normalized against the CENP-B or Hec1 signal, the Chk2 and pT383 was normalized against the CENP-A signal, and the pS331 was normalized against the Hec1 or CENP-A signal. Several kinetochore pairs per cell from a minimum of three cells per experiment from two independent experiments were analyzed for each treatment. For Cyclin B or Cyclin B-mCherry fluorescence intensities, background readings were subtracted, and Cyclin B or mCherry fluorescence for each mitotic cell was quantified by analyzing an equal image area using ImageJ (National Institutes of Health).

Mitotic indices

Cells were fixed in 4% paraformaldehyde in cytoskeleton buffer, permeabilized in 0.5% Triton X-100, stained, and examined for condensed chromatin by fluorescence microscopy. For rescue experiments in Figs. 2, 6, S2, and S4, cells were transfected with Cdk1-GFP, pEGFP-N1, Mps1-GFP^{WT}, Mps1-GFP^{1288E}, or Mad2-GFP plasmids for 24 h and treated with nocodazole plus or minus Chk2 inhibitor II or Mps1 siRNA for a further 8–12 h. Mitotic index was calculated as percentage of mitotic green cells/total green cells. For each experiment, a minimum of 100 cells per sample was analyzed.

Mps1 immunoprecipitation and kinase assay

For Mps1 immunoprecipitations, cells were lysed for 30 min in ice-cold Mps1 lysis buffer (50 mM Tris-HCl, pH 7.4, 100 mM NaCl, 0.5% NP-40, 5 mM EDTA, 5 mM EGTA, 0.2 mM PMSF, 1 μg/ml leupeptin, 40 mM sodium β-glycerophosphate, 1 mM sodium vanadate, 20 mM NaF, and 1 mM DTT) essentially as previously described (Hewitt et al., 2010). 1 mg cell lysate was incubated with 2 μg monoclonal anti-Mps1 antibody (Abcam) for 16 h followed by addition of 20 μl protein A/G PLUS-agarose beads (Santa Cruz Biotechnology, Inc.) for 1 h at 4°C. Samples were spun down and washed twice with Mps1 lysis buffer and twice with Mps1 kinase buffer (25 mM Tris-HCl, pH 7.4, 100 mM NaCl, 50 μg/ml BSA, 0.1 mM EGTA, 10 mM MgCl₂, and 2 mM DTT).

Immunoprecipitated proteins on agarose beads were included into a 20-μl reaction in Mps1 kinase buffer containing 1 μg GST-BLM (9–479), AZ3146, and 2 μCi γ-ATP. Reactions were incubated for 30 min at 30°C, stopped by addition of 10 μl 3x gel sample buffer (New England Biolabs, Inc.), and analyzed by SDS-PAGE. Radioactive labeling of the GST-BLM (9–479) substrate was determined by autoradiography.

GFP immunoprecipitation

For GFP immunoprecipitations, cells were lysed as described in the previous paragraph, lysates were incubated with 1 μg anti-GFP antibody, and immunoprecipitated proteins on agarose beads were analyzed by SDS-PAGE and Western blotting.

Myc immunoprecipitation and kinase assay

For Myc immunoprecipitations, cells were sonicated 3x for 10 s in ice-cold radioimmunoprecipitation buffer (50 mM Tris-HCl, pH 8.0, 150 mM NaCl,

1% NP-40, 0.5% deoxycholate, 0.1% SDS, 1 mM PMSF, 1 μg/ml leupeptin, 1 μg/ml aprotinin, 30 μg/ml RNase, 20 mM sodium β-glycerophosphate, and 0.3 mM sodium vanadate). 1 mg cell lysate was incubated with 0.5 μg anti-Myc antibody for 16 h followed by addition of 20 μl protein A/G PLUS-agarose beads for 1 h at 4°C. Samples were spun down and washed twice with radioimmunoprecipitation buffer, once with wash buffer (50 mM Tris-HCl, pH 8.0, 0.4 M NaCl, 1% NP-40, 0.5% deoxycholate, 1 mM PMSF, 1 μg/ml leupeptin, and 1 μg/ml aprotinin), and twice with Tris buffer (10 mM Tris-HCl, pH 7.5, 150 mM NaCl, and 0.1 mM PMSF). Immunoprecipitated proteins on agarose beads were included into a 20-μl reaction containing 1 μg histone H3, 50 mM Tris-HCl, pH 7.4, 10 mM MgCl₂, 1 mM EGTA, 1 mM DTT, 5 mM NaF, 5 mM sodium β-glycerophosphate, 50 μM sodium vanadate, and 0.1 mM ATP for 30 min at 30°C before analysis by SDS-PAGE and Western blotting using a polyclonal antibody against pH3.

Cdk1 immunoprecipitation and kinase assay

For Cdk1 immunoprecipitations, cells were sonicated 3x for 10 s in ice-cold immunoprecipitation/kinase buffer (50 mM Hepes, pH 7.5, 150 mM NaCl, 1 mM EDTA, 2.5 mM EGTA, 10% glycerol, 0.1% Tween 20, 0.1 mM PMSF, 10 μg/ml leupeptin, 10 μg/ml aprotinin, 1 mM sodium fluoride, 10 mM sodium β-glycerophosphate, and 0.1 mM sodium vanadate). 1 mg cell lysate was incubated with 0.5 μg anti-Cdk1 antibody for 16 h followed by addition of 20 μl protein A/G PLUS-agarose beads for 1 h at 4°C. Samples were spun down and washed three times with immunoprecipitation/kinase buffer and three times with kinase buffer (50 mM Hepes, pH 7.5, 50 mM NaCl, 10 mM MgCl₂, and 1 mM DTT).

Immunoprecipitated proteins on agarose beads were included into a 20-μl reaction in kinase buffer containing 1 μg histone H1, 50 μM ATP, and 2 μCi γ-ATP for 30 min at 30°C before analysis by SDS-PAGE. Radioactive labeling of the H1 substrate was determined by autoradiography.

Chk2 kinase assay

For Chk2 in vitro kinase assays, 0.5 μg recombinant Chk2 was incubated with 1 μg protein substrate in 20 μl kinase buffer (50 mM Hepes, pH 8.0, 2.5 mM EDTA, 10 mM MgCl₂, 1 mM DTT, 10 mM sodium β-glycerophosphate, 0.1 mM sodium vanadate, 0.1 mM PMSF, 1 mM sodium fluoride, 100 μM ATP, and 2 μCi γ-ATP) for 30 min at 30°C before analysis by SDS-PAGE and autoradiography. Where appropriate, 364 ng Chk2 inhibitor II (EMD Millipore) was included in the kinase reaction.

Western blotting

Cells were lysed in ice-cold whole cell extract buffer (20 mM Hepes, 5 mM EDTA, 10 mM EGTA, 0.4 M KCl, 0.4% Triton X-100, 10% glycerol, 5 mM NaF, 1 mM DTT, 5 μg/ml leupeptin, 50 μg/ml PMSF, 1 mM benzamidine, 5 μg/ml aprotinin, and 1 mM Na₃VO₄) for 30 min on ice. Lysates were cleared by centrifugation at 15,000 g for 10 min, analyzed by SDS-PAGE, and transferred onto nitrocellulose membrane (Santa Cruz Biotechnology, Inc.).

Densitometry

Densitometric analysis of the bands was performed using ImageJ.

Statistical analysis

The p-values were calculated using the Student's *t* test.

Online supplemental material

Fig. S1 shows microtubule and Nbs1 stainings, mitotic index analysis in BE, HCT116, or CHO cells after treatment with Chk2 inhibitor II, and human Mps1 kinase activity in the presence of various concentrations of the Mps1 inhibitor AZ3146. Fig. S2 shows that Chk2-deficient cells exhibit Cdk1-Y15 phosphorylation and Mps1 degradation in high nocodazole. Fig. S3 shows Chk2-pT383 staining in unperturbed prophase, Aurora B-S331 phosphorylation in cells treated with taxol or low nocodazole, Myc-Aurora B expression levels, Myc-associated catalytic activity in CHO cell lines, and CHO Mps1 kinase activity in the presence of various concentrations of AZ3146. Fig. S4 shows that Chk2 inhibition reduces Mps1 localization to kinetochores in high nocodazole. Fig. S5 shows that Chk2 is dispensable for Mad2 localization to kinetochores in unperturbed late pro-metaphase. Video 1 shows control cells arrested in mitosis in the presence of high nocodazole. Video 2 shows Chk2-deficient cells decondensing their chromosomes and forming micronuclei in the presence of high nocodazole. Online supplemental material is available at <http://www.jcb.org/cgi/content/full/jcb.201310071/DC1>.

We thank G. Sourvinos for helping with the time lapse. We also thank T. Fukagawa, D. Gillespie, A. Musacchio, R. Muschel, S. Sengupta, and S. Taylor for generously sharing reagents.

This work was funded by the Association for International Cancer Research.

The authors declare no competing financial interests.

Submitted: 15 October 2013

Accepted: 4 April 2014

References

- Abrieu, A., L. Magnaghi-Jaulin, J.A. Kahana, M. Peter, A. Castro, S. Vigneron, T. Lorca, D.W. Cleveland, and J.C. Labbé. 2001. Mps1 is a kinetochore-associated kinase essential for the vertebrate mitotic checkpoint. *Cell*. 106:83–93. [http://dx.doi.org/10.1016/S0092-8674\(01\)00410-X](http://dx.doi.org/10.1016/S0092-8674(01)00410-X)
- Ahn, J., and C. Prives. 2002. Checkpoint kinase 2 (Chk2) monomers or dimers phosphorylate Cdc25C after DNA damage regardless of threonine 68 phosphorylation. *J. Biol. Chem.* 277:48418–48426. <http://dx.doi.org/10.1074/jbc.M208321200>
- Ahn, J.Y., X. Li, H.L. Davis, and C.E. Canman. 2002. Phosphorylation of threonine 68 promotes oligomerization and autophosphorylation of the Chk2 protein kinase via the forkhead-associated domain. *J. Biol. Chem.* 277:19389–19395. <http://dx.doi.org/10.1074/jbc.M200822200>
- Brito, D.A., and C.L. Rieder. 2006. Mitotic checkpoint slippage in humans occurs via cyclin B destruction in the presence of an active checkpoint. *Curr. Biol.* 16:1194–1200. <http://dx.doi.org/10.1016/j.cub.2006.04.043>
- Chen, Y., and R.Y. Poon. 2008. The multiple checkpoint functions of CHK1 and CHK2 in maintenance of genome stability. *Front. Biosci.* 13:5016–5029.
- Chow, J.P., R.Y. Poon, and H.T. Ma. 2011. Inhibitory phosphorylation of cyclin-dependent kinase 1 as a compensatory mechanism for mitosis exit. *Mol. Cell. Biol.* 31:1478–1491. <http://dx.doi.org/10.1128/MCB.00891-10>
- Cimini, D. 2008. Merotelic kinetochore orientation, aneuploidy, and cancer. *Biochim. Biophys. Acta*. 1786:32–40.
- Ditchfield, C., V.L. Johnson, A. Tighe, R. Ellston, C. Haworth, T. Johnson, A. Mortlock, N. Keen, and S.S. Taylor. 2003. Aurora B couples chromosome alignment with anaphase by targeting BubR1, Mad2, and Cenp-E to kinetochores. *J. Cell Biol.* 161:267–280. <http://dx.doi.org/10.1083/jcb.200208091>
- Fletcher, L., Y. Cheng, and R.J. Muschel. 2002. Abolishment of the Tyr-15 inhibitory phosphorylation site on cdc2 reduces the radiation-induced G(2) delay, revealing a potential checkpoint in early mitosis. *Cancer Res.* 62:241–250.
- Foley, E.A., and T.M. Kapoor. 2013. Microtubule attachment and spindle assembly checkpoint signalling at the kinetochore. *Nat. Rev. Mol. Cell Biol.* 14:25–37. <http://dx.doi.org/10.1038/nrm3494>
- Gavet, O., and J. Pines. 2010. Progressive activation of CyclinB1-Cdk1 coordinates entry to mitosis. *Dev. Cell.* 18:533–543. <http://dx.doi.org/10.1016/j.devcel.2010.02.013>
- Giunta, S., R. Belotserkovskaya, and S.P. Jackson. 2010. DNA damage signaling in response to double-strand breaks during mitosis. *J. Cell Biol.* 190:197–207. <http://dx.doi.org/10.1083/jcb.20091156>
- Hewitt, L., A. Tighe, S. Santaguida, A.M. White, C.D. Jones, A. Musacchio, S. Green, and S.S. Taylor. 2010. Sustained Mps1 activity is required in mitosis to recruit O-Mad2 to the Mad1–C-Mad2 core complex. *J. Cell Biol.* 190:25–34. <http://dx.doi.org/10.1083/jcb.201002133>
- Jelluma, N., A.B. Brenkman, N.J. van den Broek, C.W. Cruijsen, M.H. van Osch, S.M. Lens, R.H. Medema, and G.J. Kops. 2008. Mps1 phosphorylates Borealin to control Aurora B activity and chromosome alignment. *Cell*. 132:233–246. <http://dx.doi.org/10.1016/j.cell.2007.11.046>
- Kabeche, L., and D.A. Compton. 2012. Checkpoint-independent stabilization of kinetochore-microtubule attachments by Mad2 in human cells. *Curr. Biol.* 22:638–644. <http://dx.doi.org/10.1016/j.cub.2012.02.030>
- Kapoor, T.M., T.U. Mayer, M.L. Coughlin, and T.J. Mitchison. 2000. Probing spindle assembly mechanisms with monastrol, a small molecule inhibitor of the mitotic kinesin, Eg5. *J. Cell Biol.* 150:975–988. <http://dx.doi.org/10.1083/jcb.150.5.975>
- Lampson, M.A., and T.M. Kapoor. 2005. The human mitotic checkpoint protein BubR1 regulates chromosome-spindle attachments. *Nat. Cell Biol.* 7:93–98. <http://dx.doi.org/10.1038/ncb1208>
- Lee, C.H., and J.H. Chung. 2001. The hCd1 (Chk2)-FHA domain is essential for a chain of phosphorylation events on hCd1 that is induced by ionizing radiation. *J. Biol. Chem.* 276:30537–30541. <http://dx.doi.org/10.1074/jbc.M104414200>
- Leng, M., D.W. Chan, H. Luo, C. Zhu, J. Qin, and Y. Wang. 2006. MPS1-dependent mitotic BLM phosphorylation is important for chromosome stability. *Proc. Natl. Acad. Sci. USA*. 103:11485–11490. <http://dx.doi.org/10.1073/pnas.0601828103>
- Maciejowski, J., K.A. George, M.E. Terret, C. Zhang, K.M. Shokat, and P.V. Jallepalli. 2010. Mps1 directs the assembly of Cdc20 inhibitory complexes during interphase and mitosis to control M phase timing and spindle checkpoint signaling. *J. Cell Biol.* 190:89–100. <http://dx.doi.org/10.1083/jcb.201001050>
- Magidson, V., C.B. O'Connell, J. Lon arek, R. Paul, A. Mogilner, and A. Khodjakov. 2011. The spatial arrangement of chromosomes during pro-metaphase facilitates spindle assembly. *Cell*. 146:555–567. <http://dx.doi.org/10.1016/j.cell.2011.07.012>
- Malureanu, L., K.B. Jeganathan, F. Jin, D.J. Baker, J.H. van Ree, O. Gullon, Z. Chen, J.R. Henley, and J.M. van Deursen. 2010. Cdc20 hypomorphic mice fail to counteract de novo synthesis of cyclin B1 in mitosis. *J. Cell Biol.* 191:313–329. <http://dx.doi.org/10.1083/jcb.201003090>
- Matson, D.R., P.B. Demirel, P.T. Stukenberg, and D.J. Burke. 2012. A conserved role for COMA/CENP-H/I/N kinetochore proteins in the spindle checkpoint. *Genes Dev.* 26:542–547. <http://dx.doi.org/10.1101/gad.184184.111>
- McGowan, C.H., and P. Russell. 1993. Human Wee1 kinase inhibits cell division by phosphorylating p34cdc2 exclusively on Tyr15. *EMBO J.* 12:75–85.
- Minshull, J., A. Straight, A.D. Rudner, A.F. Dernburg, A. Belmont, and A.W. Murray. 1996. Protein phosphatase 2A regulates MPF activity and sister chromatid cohesion in budding yeast. *Curr. Biol.* 6:1609–1620. [http://dx.doi.org/10.1016/S0960-9822\(02\)70784-7](http://dx.doi.org/10.1016/S0960-9822(02)70784-7)
- Mueller, P.R., T.R. Coleman, and W.G. Dunphy. 1995a. Cell cycle regulation of a *Xenopus* Wee1-like kinase. *Mol. Biol. Cell*. 6:119–134. <http://dx.doi.org/10.1091/mbc.6.1.119>
- Mueller, P.R., T.R. Coleman, A. Kumagai, and W.G. Dunphy. 1995b. Myt1: a membrane-associated inhibitory kinase that phosphorylates Cdc2 on both threonine-14 and tyrosine-15. *Science*. 270:86–90. <http://dx.doi.org/10.1126/science.270.5233.86>
- Nezi, L., and A. Musacchio. 2009. Sister chromatid tension and the spindle assembly checkpoint. *Curr. Opin. Cell Biol.* 21:785–795. <http://dx.doi.org/10.1016/j.ceb.2009.09.007>
- Peters, J.M. 2002. The anaphase-promoting complex: proteolysis in mitosis and beyond. *Mol. Cell.* 9:931–943. [http://dx.doi.org/10.1016/S1097-2765\(02\)00540-3](http://dx.doi.org/10.1016/S1097-2765(02)00540-3)
- Petsalaki, E., and G. Zachos. 2013. Chk1 and Mps1 jointly regulate correction of merotelic kinetochore attachments. *J. Cell Sci.* 126:1235–1246. <http://dx.doi.org/10.1242/jcs.119677>
- Petsalaki, E., T. Akoumianakian, E.J. Black, D.A. Gillespie, and G. Zachos. 2011. Phosphorylation at serine 331 is required for Aurora B activation. *J. Cell Biol.* 195:449–466. <http://dx.doi.org/10.1083/jcb.201104023>
- Posch, M., G.A. Khoudoli, S. Swift, E.M. King, J.G. Deluca, and J.R. Swedlow. 2010. Sds22 regulates aurora B activity and microtubule-kinetochore interactions at mitosis. *J. Cell Biol.* 191:61–74. <http://dx.doi.org/10.1083/jcb.200912046>
- Rainey, M.D., E.J. Black, G. Zachos, and D.A. Gillespie. 2008. Chk2 is required for optimal mitotic delay in response to irradiation-induced DNA damage incurred in G2 phase. *Oncogene*. 27:896–906. <http://dx.doi.org/10.1038/sj.onc.1210702>
- Santaguida, S., A. Tighe, A.M. D'Alise, S.S. Taylor, and A. Musacchio. 2010. Dissecting the role of MPS1 in chromosome biorientation and the spindle checkpoint through the small molecule inhibitor reversine. *J. Cell Biol.* 190:73–87. <http://dx.doi.org/10.1083/jcb.201001036>
- Santaguida, S., C. Vernieri, F. Villa, A. Ciliberto, and A. Musacchio. 2011. Evidence that Aurora B is implicated in spindle checkpoint signalling independently of error correction. *EMBO J.* 30:1508–1519. <http://dx.doi.org/10.1038/embj.2011.70>
- Saurin, A.T., M.S. van der Waal, R.H. Medema, S.M. Lens, and G.J. Kops. 2011. Aurora B potentiates Mps1 activation to ensure rapid checkpoint establishment at the onset of mitosis. *Nat. Commun.* 2:316. <http://dx.doi.org/10.1038/ncomms1319>
- Schwarz, J.K., C.M. Lovly, and H. Piwnica-Worms. 2003. Regulation of the Chk2 protein kinase by oligomerization-mediated cis- and trans-phosphorylation. *Mol. Cancer Res.* 1:598–609.
- Srivastava, V., P. Modi, V. Tripathi, R. Mudgal, S. De, and S. Sengupta. 2009. BLM helicase stimulates the ATPase and chromatin-remodeling activities of RAD54. *J. Cell Sci.* 122:3093–3103. <http://dx.doi.org/10.1242/jcs.051813>
- Stolz, A., N. Ertch, A. Kienitz, C. Vogel, V. Schneider, B. Fritz, R. Jacob, G. Dittmar, W. Weichert, I. Petersen, and H. Bastians. 2010. The CHK2-BRCA1 tumour suppressor pathway ensures chromosomal stability in human somatic cells. *Nat. Cell Biol.* 12:492–499. <http://dx.doi.org/10.1038/ncb2051>

- Tang, Z., T.R. Coleman, and W.G. Dunphy. 1993. Two distinct mechanisms for negative regulation of the Wee1 protein kinase. *EMBO J.* 12: 3427–3436.
- Taylor, S.S., D. Hussein, Y. Wang, S. Elderkin, and C.J. Morrow. 2001. Kinetochore localisation and phosphorylation of the mitotic checkpoint components Bub1 and BubR1 are differentially regulated by spindle events in human cells. *J. Cell Sci.* 114:4385–4395.
- Tsvetkov, L., X. Xu, J. Li, and D.F. Stern. 2003. Polo-like kinase 1 and Chk2 interact and co-localize to centrosomes and the midbody. *J. Biol. Chem.* 278:8468–8475. <http://dx.doi.org/10.1074/jbc.M211202200>
- van der Waal, M.S., R.C. Hengeveld, A. van der Horst, and S.M. Lens. 2012. Cell division control by the Chromosomal Passenger Complex. *Exp. Cell Res.* 318:1407–1420. <http://dx.doi.org/10.1016/j.yexcr.2012.03.015>
- van Vugt, M.A., A.K. Gardino, R. Linding, G.J. Osthimer, H.C. Reinhardt, S.E. Ong, C.S. Tan, H. Miao, S.M. Keezer, J. Li, et al. 2010. A mitotic phosphorylation feedback network connects Cdk1, Plk1, 53BP1, and Chk2 to inactivate the G(2)/M DNA damage checkpoint. *PLoS Biol.* 8:e1000287. <http://dx.doi.org/10.1371/journal.pbio.1000287>
- Yeh, Y.H., Y.F. Huang, T.Y. Lin, and S.Y. Shieh. 2009. The cell cycle checkpoint kinase CHK2 mediates DNA damage-induced stabilization of TTK/hMps1. *Oncogene.* 28:1366–1378. <http://dx.doi.org/10.1038/onc.2008.477>
- Zachos, G., E.J. Black, M. Walker, M.T. Scott, P. Vagnarelli, W.C. Earnshaw, and D.A. Gillespie. 2007. Chk1 is required for spindle checkpoint function. *Dev. Cell.* 12:247–260. <http://dx.doi.org/10.1016/j.devcel.2007.01.003>